Shoulder

5

Daniel R. Lueders, Alexander R. Lloyd,
and Allison N. Schroeder

Long Head of the Biceps Brachii

Anatomy and Ultrasound Evaluation

The biceps brachii has two heads – short and long – which act together to flex the shoulder and elbow and assist with forearm supination. The long head of the biceps brachii (LHBB) originates on the supraglenoid tubercle, rim of the glenoid, superior glenoid, and the joint capsule. The short head of the biceps brachii (SHBB) originates at the coracoid process of the scapula. These heads merge at the level of the pectoralis major and insert on the radial tubercle and as the lacertus fibrosus onto the deep fascia of the forearm. The LHBB follows a curvilinear course from its origin and passes through the rotator interval formed by the superior border subscapularis inferiorly, anterior border of the supraspinatus superiorly, and the base of the coracoid process medially. The coracohumeral ligament and the glenohumeral ligament also overlie the LHBB within this interval and restrain medial movement. The LHBB is encased in a synovial sheath that communicates with the glenohumeral joint.

D. R. Lueders (✉) · A. N. Schroeder
University of Pittsburgh Medical Center,
Pittsburgh, PA, USA
e-mail: luedersdr2@upmc.edu;
aschroe1@alumni.nd.edu

A. R. Lloyd
University of Pittsburgh Medical Center,
Department of PM&R, Pittsburgh, PA, USA

For ultrasound evaluation of the LHBB, the patient should rest their arm adducted to the side and in neutral to slight external rotation. This brings the tendon anteriorly and allows the sonographer to trace the biceps tendon from its distal point at the pectoralis major to its proximal portion within the rotator interval. Failing to do this and leaving the patient internally rotated can hinder initial localization of the tendon and can prevent comfortable positioning of the probe to allow for optimal visualization of the tendon. The LHBB is generally superficial even in obese patients, making a high-frequency linear probe the best choice for exam. Decreasing both depth and focal zone to evaluate the proximal position of the tendon can improve visualization. The probe should be carefully adjusted to achieve a perpendicular view of the tendon and to eliminate artifact from anisotropy. This may be challenging, given the curvilinear path of the tendon, and requires constant reorientation of the probe. Maintaining a discrete visualization of the cortex of the humerus as a well-defined, hyperechoic structure underlying the biceps tendon indicates the probe is perpendicular to the contour of the bone and can assist with proper probe alignment.

The scan begins with the transducer in the transverse plane on the anterior aspect of the proximal shoulder. The LHBB tendon is identified in short axis within the bicipital groove of the humerus. (Fig. 5.1) The tendon should be scanned

Y. El Miedany (ed.), *Musculoskeletal Ultrasound-Guided Regenerative Medicine*,
https://doi.org/10.1007/978-3-030-98256-0_5

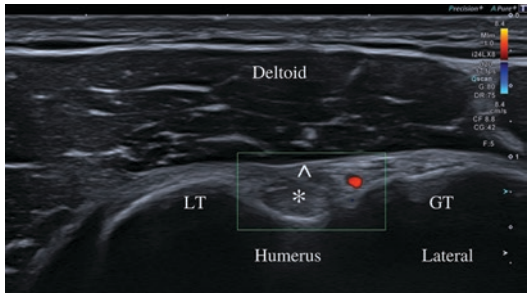

Fig. 5.1 Transverse view of the biceps brachii long head tendon in the intertubercular groove, or biceps tunnel. The biceps tendon (*) is seen as a dense, homogenous hyperechoic ovoid structure sitting between the humeral lesser tuberosity (LT) and greater tuberosity (GT). The hyperechoic fibrillar-appearing transverse humeral ligament (^) sits superficial to the biceps long head tendon and secures it within the biceps tunnel superior to the epiphyseal line

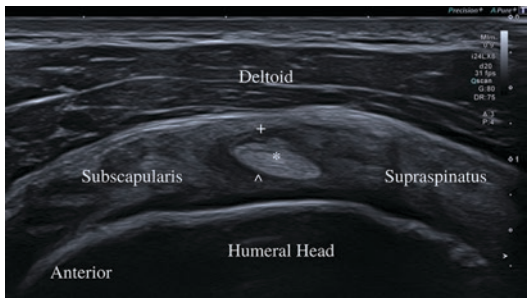

Fig. 5.2 Transverse view of the biceps brachii long head tendon at the rotator interval. The biceps tendon (star) is seen as a dense, homogenous hyperechoic ovoid structure sitting on the humeral head and deep to deltoid. The anterior, or leading edge, of supraspinatus forms the posterior margin of the rotator interval, while the cephalad-most fibers of subscapularis form the anterior margin of the rotator interval. The superficial rotator interval is comprised of the coracohumeral ligament (+), and the deep rotator interval is bordered by the superior glenohumeral ligament (^)

proximally through the rotator interval as this is a common site of pathology. (Fig. 5.2) The LHBB tendon has an oval shape proximal to the bicipital groove and migrates medially toward the glenoid at this point. This should not be confused for tendon subluxation. The tendon generally cannot be followed all the way to its origin on the supraglenoid tubercle because of the overlying bony anatomy. Some fibers may be seen blending with the surrounding tissues at this level as they move to their origin on the capsule and labrum.

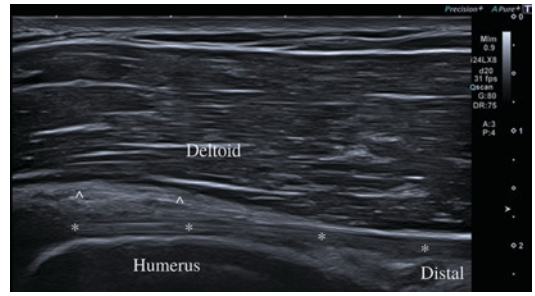

Fig. 5.3 Longitudinal view of the biceps brachii long head tendon in the intertubercular groove, or biceps tunnel. The biceps (*) courses adjacent to the humerus at the biceps tunnel, and the transverse humeral ligament (^) can be seen superficial to the tendon securing it in place

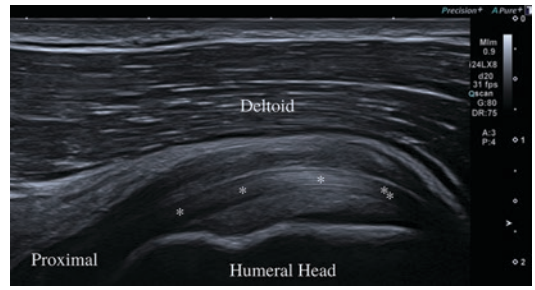

Fig. 5.4 Longitudinal view of the biceps brachii long head tendon (*) adjacent to the humeral head and deep to deltoid

The tendon should then be followed inferiorly to the level of its myotendinous junction just caudad from the traversing pectoralis major tendon, which is visualized emerging in long axis medial to the biceps long head tendon and subsequently traversing superficial to biceps tendon to insert on the lateral aspect of the humerus. Doppler evaluation should also be performed to identify an ascending branch of the anterior circumflex artery, which courses lateral to the LHBB tendon in the bicipital groove. Also of note, the transverse humeral ligament overlies the bicipital groove and appears as a thin, hyperechoic band superficial to LHBB tendon. The tendon should then be evaluated in a long axis view (Fig. 5.3). Maintaining this view over the entire course of the tendon can be challenging, particularly as the tendon curves into the rotator interval (Fig. 5.4). Increased pressure on the distal end of the transducer may assist with bringing the tendon paral-

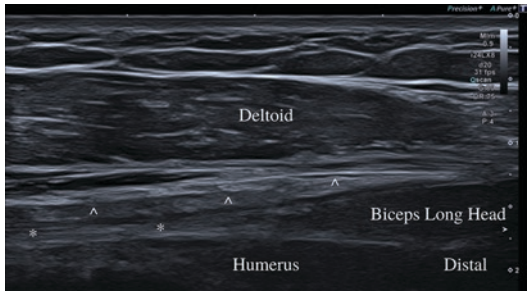

Fig. 5.5 Longitudinal view of the biceps brachii long head tendon (*) at its myotendinous junction distally. The broad, flat tendon of pectoralis major (^) is visualized superficial to the biceps tendon just proximal from the biceps myotendinous junction

lel to the plane of the transducer. The tendon should again be scanned from proximal to distal to evaluate for pathology at the myotendinous junction (Fig. 5.5).

Pathology

LHBB tendon pathology is seen most commonly within the first 3.5 cm from the tendon origin and within, or close to, the rotator interval [1]. Chronic degenerative injury to the LHBB may result in tendinosis. This phenomenon represents the noninflammatory mucoid degeneration and chondroid metaplasia of chronically injured tendons [2]. Tendinosis manifests as hypoechoic defects with changes to the fibrillar architecture of the tendon that give it an ill-defined heterogenous appearance [3]. Concomitant thickening of the tendon and Doppler flow may also be seen in the abnormal areas [3].

Anechoic clefts or irregularities in the superficial contour of the biceps tendon may indicate partial-thickness tearing [4]. Full-thickness tearing results in the complete absence tendon in the bicipital groove due to its retraction distally into the arm. The full extent of the bicipital groove should be evaluated distally to locate the retracted stump of the tendon. Of note, the collapsed bicipital tendon sheath may appear as a hyperechoic fascial structure within the bicipital groove and should not be mistaken for the biceps tendon [5]. Reactive effusion and debris can also fill the vacancy of the ruptured tendon and mimic an abnormal tendon [6].

The tendon sheath of the LHBB usually contains minimal to no fluid. However, because of the tendon sheath that communicates with the glenohumeral joint space, a glenohumeral joint effusion greater than 5 mL can result in peritendinous extravasation of the effusion down the tendon sheath to the level of the bicipital groove [7]. As a result, effusion within the LHBB sheath may indicate both LHBB tendon and glenohumeral joint pathology. Fluid resulting from glenohumeral effusion is usually evenly distributed circumferentially around and along the LHBB tendon and is not focally tender. This is in comparison to focal tenosynovitis, which is often painful with sonopalpation and demonstrates focal fluid deposition. Areas of tenosynovitis may also demonstrate hyperemia that can be seen with Doppler imaging. The presence of the anterior circumflex artery lateral to the tendon should not be confused with hyperemia. Fluid in the tendon sheath may finally be associated with rotator cuff tear. This is particularly the case when an effusion of the subacromial/subdeltoid bursa is also present [7, 8].

Subluxation or dislocation of the LHBB tendon occurs in the medial direction and generally results from disruption of the coracohumeral ligament. Suspicion for subluxation or complete dislocation of the tendon should arise when the tendon is not seen in the bicipital groove. During subluxation, the tendon can be observed subluxating medially out of the bicipital groove with external rotation and relocating back into the bicipital groove with internal rotation. When dislocation has occurred, the tendon has permanently migrated medially and may be difficult to visualize. LHBB subluxation or dislocation should not be confused with a complete tear of the tendon, which may similarly show an empty bicipital groove. To differentiate between the two, examiners must scan distally to visualize the most proximal portion of the tendon that can be visualized. This should then be followed more proximally. An abnormal tendon course that courses medial to the humerus indicates subluxation or dislocation, while discontinuity indicates rupture of the tendon.

While LHBB tendon pathology may be focal and isolated, it can be an indicator of glenohumeral joint or rotator cuff pathology [7–9]. Even damage to the LHBB tendon itself may reflect abnormal biomechanics within the shoulder triggered by pathology elsewhere in the rotator cuff [9].

Interventional Procedures

Limited evidence exists for dedicated regenerative procedures performed at the LHBB tendon. Prolotherapy protocols involving injection of the proximal biceps tendon almost always do so as part of a larger protocol for rotator cuff disease with multiple other tendons injected [10, 11]. It's difficult to make definitive conclusions as a result, because improvements in pain or function may have been related to effects at other locations. No studies have been performed with prolotherapy on isolated biceps tendon pathology.

With reference to PRP, a single pilot study evaluated the effect of PRP injections to the LHBB tendon in eight spinal cord injured patients with good overall outcomes [12]. Beyond this, no data was found about PRP injections for isolated proximal biceps tendon pathology. As previously mentioned, the biceps tendon may be affected by significant pathology of the supraspinatus and subscapularis tendons through disruption of the rotator interval and rotator pulley that may lead to tendon dysfunction [13]. Additionally, there is likely some bursal communication between the subacromial-subdeltoid bursa and the biceps tendon sheath when significant rotator cuff tearing is present [7]. However, use based on this evidence is largely speculative.

No systematic studies have been performed examining the effects of mesenchymal stem cells or hyaluronic acid on the biceps tendon.

Injection Approach #1

- Patient positioning – Supine.
- Transducer selection – High-frequency linear array transducer (>10MHz)
- Transducer position – Short axis to the long head of the biceps tendon at the intertubercular groove
- Needle selection – 25–27-gauge 1.5–2.5-inch needle, depending on body habitus
- Injectate selection – Anesthetize with local anesthetic. Inject with 5mL or less of volume including steroid, prolotherapy, or orthobiologic therapy. Volumes of 5mL or more commonly enter the glenohumeral joint and may be used for adhesive capsulitis [7].
- Needle trajectory and target – In-plane, lateral to medial, target is just superficial to the tendon within the sheath to ensure the safety of the ascending artery from the anterior humoral circumflex artery.
- Accuracy – Ultrasound-guided injections of the biceps tendon sheath are significantly more accurate than palpation-guided injections. Many practitioners struggle to accurately identify the correct location of the biceps tendon with palpation, leading to frequent needle placement error [14]. Recent comparative studies have found ultrasound-guided injections to be between 85% and 100% accurate with superior effectiveness [15–17]. Palpation-guided injections range in accuracy from 26% to 68% (Hashiuchi et al. [16]; Yiannakopoulos et al. [17]).
- Pearls/Pitfalls
  - The lesser tuberosity can be used as a backstop for the needle trajectory to facilitate proper placement
  - Injectate should flow easily and disseminate within the tendon sheath. Focal collection of the fluid indicates the needle is either outside of the sheath or within the tendon.
  - The anterior circumflex humeral artery, which typically lies lateral to the tendon, should always be visualized with Doppler prior to the injection and avoided during the procedure.

Injection approach #2

- Patient positioning – Supine
- Transducer selection – High-frequency linear array transducer (>10MHz)
- Transducer position – Long axis to the long head of the biceps tendon at the intertubercular groove

- Needle selection – 25–2-gauge 1.5–2.5-inch needle depending on body habitus
- Injectate selection – Same as above
- Needle trajectory and target – In-plane, inferior to superior, target is just superficial to the tendon within the sheath
- Accuracy – As above
- Pearls/Pitfalls
  - This approach provides another option in the event that approach #1 is not possible.
  - While this approach allows for a longer tendon target, it lacks simultaneous visualization of the anterior circumflex humeral artery and lacks a bony backstop if the injector misjudges the needle depth.

Supraspinatus Tendon

Anatomy and Ultrasound Evaluation

The supraspinatus tendon originates from the supraspinous fossa of the scapula. It courses superolaterally to pass under the acromion and over the superior aspect of the glenohumeral joint before inserting on the middle and superior facet of the greater tuberosity. The supraspinatus muscle has a complex architecture that permits it to provide significant stability to the humeral head during rotation and abduction at a variety of angles. This includes a ventral or anterior portion that inserts more anteriorly on the greater tuberosity and acts as an internal rotator, as well as a posterior portion that inserts posteriorly on the greater tuberosity and serves to abduct the shoulder [18, 19]. Each of these portions is subdivided into superficial, middle, and deep portions, each with its own insertion [18]. This complex architecture with resulting complex movement is thought to contribute to its susceptibility to injury [18]. The supraspinatus musculature and tendon are separated from surrounding musculature and bony prominences by the subacromial-subdeltoid (SASD) bursa, which functions to facilitate movement of the tendon. The SASD bursa is described separately. As the supraspinatus courses laterally toward its insertion, the supraspinatus forms the posterosuperior border of the rotator interval, which surrounds the proximal portion of the LHBB.

Ultrasound evaluation of the medial, proximal supraspinatus tendon is obscured by the bony acromion at rest in a neutral position. Placing the patient in a Crass position (hand behind the back with shoulder extension and internal rotation) or modified-Crass position (hand on the hip with shoulder in extension) angles the greater tuberosity anteriorly, pulling a larger portion of the supraspinatus out from underneath the acromion. The Crass position may obscure the rotator interval because of the internal rotation and be painful for patients with pathology [5]. The modified Crass is more commonly used as a result, but it should be noted that this position may overestimate the size of tendon tears [20]. It should be noted that part of the tendon will always be obscured by the coracoacromial arch and the supraspinatus should be evaluated to the maximal extent possible posterior and anterior to the acromial arch, recognizing the inherent limitations presented by the overlying bony architecture.

The supraspinatus tendon is superficial and can generally be imaged with a high-frequency linear probe within a few centimeters of the skin surface. The probe is placed over the superior and anterior aspect of the shoulder in a coronal oblique plane with the medial end of the transducer pointed towards the patient's ear. This will show the supraspinatus tendon in a long axis view (Fig. 5.6). The insertion of the supraspinatus tendon classically has a convex "bird's beak"

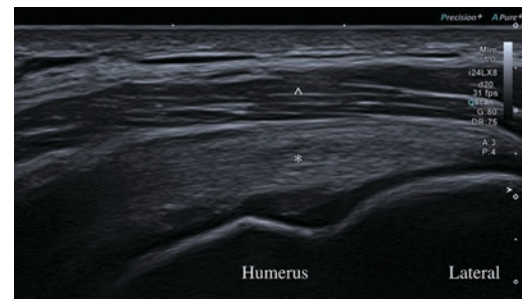

Fig. 5.6 Longitudinal view of the insertional supraspinatus (*) onto humerus. Deltoid (^) is superficial to supraspinatus

appearance as it inserts on the greater tuberosity. In this view, the greater tuberosity, bursal, and articular surfaces of the tendon can be evaluated for pathology. The tendon will appear fibrillar and hyperechoic with fibrocartilage often seen deep to the tendon over the facets. Hypoechoic articular cartilage may also be seen over the humeral head. Heel-toe of the transducer should be used over the insertion of the supraspinatus to eliminate anisotropy caused by the downward curve of the tendon at the insertion on the humerus.

The footprint of the supraspinatus covers approximately 25 mm of the greater tuberosity, and the entire footprint should be scanned [21]. The boundaries of the supraspinatus can be identified by scanning anteriorly until the biceps tendon is seen within the rotator interval and posteriorly until the infraspinatus comes into oblique view. The tendon should then be scanned superiorly in long axis until the acromion is encountered. The SASD bursa may be seen as a thin, hypoechoic line overlying the supraspinatus tendon, although it is collapsed in those without pathology and may be difficult to visualize.

Once long-axis evaluation has been completed, the transducer should be rotated 90° to evaluate the tendon in short axis (Fig. 5.7). Scanning should be started at the level of the humeral head with the proximal tendon in view over underlying articular cartilage. The tendon thickness generally measures 5–6 mm in thickness 1–2 cm from the insertion and may vary by approximately 0.5 mm between men and women

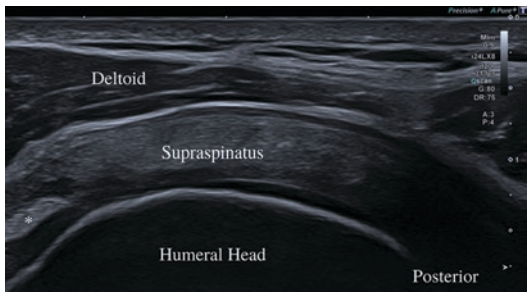

Fig. 5.7 Transverse view of the supraspinatus insertion onto humerus. The long head biceps brachii tendon (*) is visualized at the rotator interval and leading anterior edge of supraspinatus

[22–24]. As the tendon is scanned distally, it will thin as the articular portion of the humerus gives way to the more angulated facets of the greater tuberosity. The supraspinatus will insert on the superior and superior half of the middle facet. The infraspinatus will also be seen inserting onto the middle facet at this level and the fibers of both tendons often mingle at this level, making a definitive differentiation difficult. As with the long-axis portion of the scan, the transducer should be translated anteriorly until the biceps tendon is visualized within the rotator interval and posteriorly until the infraspinatus is viewed to ensure the entire footprint has been evaluated.

Dynamic evaluation is then performed to evaluate for any visible signs of subacromial impingement. With the supraspinatus footprint and the acromion in view, the patient should slowly abduct and adduct the shoulder. The supraspinatus will be observed passing underneath the acromion. The sonographer should observe for bunching of bursal tissue against the acromion, collecting fluid at the edge of the acromion representing an effusion in the bursa, or correspondence of pain with this movement.

The musculature of the supraspinatus can be visualized posteriorly for echotexture changes that may suggest muscle pathology such as denervation or disuse. Short-axis panoramic views of the muscle can allow comparison to the infraspinatus and teres minor for reference. The musculature should have a “starry sky” appearance with a largely hypoechoic echotexture interspersed with hyperechoic connective tissue. Increased hyperechogenicity should raise concern for underlying fatty or fibrous infiltration. The musculature can be traced into the tendon up until its passage under the acromion.

The deltoid musculature is also commonly viewed during diagnostic scans in this area, although dedicated diagnostic scanning is far less common than imaging of the rotator cuff. This is largely based on the low levels of pathology seen in the deltoid relative to the muscles of the rotator cuff. The muscle originates on the lateral third of the clavicle, the acromion, and on the spine of scapula. It inserts onto the anterolateral surface of the humerus. Because of its broad origins, the

deltoid muscle assists with a variety of actions around the shoulder, including flexion, extension, internal rotation, external rotation, and abduction, although abduction is its main action. It is supplied by the axillary nerve and may show signs of denervation – atrophy, fibrosis, or fatty infiltration – in cases of axillary nerve injury The muscle may also be injured by direct blow resulting in contusion or muscle injury, which can also be visualized under ultrasound.

Pathology

The supraspinatus tendon is the most commonly torn tendon in the rotator cuff [25]. Ultrasound has been shown in several meta-analyses to be at least 90% specific and as good as MRI and potentially MR arthrogram in evaluating tearing of the tendon [26, 27]. Degenerative tears are frequently seen posterior to the biceps tendon near the junction of the supraspinatus and infraspinatus tendons [28]. The anterior supraspinatus tendon at the articular-sided footprint is also commonly affected, and concomitant cortical irregularity representing chronic injury may be seen [25]. Acute tears tend to occur more proximally and often lack the cortical irregularity seen in degenerative tears [5].

Tears are hypoechoic or anechoic areas within the substance of the tendon. Tears are described as partial- or full-thickness involving part of or the entire thickness of the tendon. Full-thickness tears appear as well-defined, hypoechoic, or anechoic disruptions in the fibrillar architecture of the tendon and may only affect part of the width of the tendon. Smaller tears may not change the overall shape of the tendon, while larger tears can lead to tendon volume loss, which flattens the typical convex appearance of the tendon [5]. Mixed hypoechoic and hyperechoic components can occur when a portion of the torn residual tendon is surrounded by fluid within the tear [29]. A complete tear is described as a full-width, full-thickness tear. Some partial-thickness tears may be difficult to evaluate based on their location or orientation, and secondary signs can be used to deduce underlying pathology. These signs include cortical irregularity at the footprint, effusion seen in the SASD bursa, a glenohumeral joint effusion, or a cartilage interface sign (hyperechoic line over the surface of the articular cartilage under the contour of the supraspinatus tendon) [3].

The location of a partial-thickness tear should also be defined as intrasubstance, bursal-sided, or articular-sided. An intrasubstance tear occurs within the tendon and does not extend to a surface of the tendon. Bursal-sided tears lead to loss of superficial fibers on the surface of the tendon, causing thinning of the tendon. The surrounding deltoid muscle and SASD bursa may then dip into this defect, causing loss of the typical convex appearance of the tendon. This is less common in articular-sided tears, because the cortical and articular surfaces underlying the tendon preserve the convex appearance of the tendon.

Chronic degeneration of the supraspinatus can result in tendinosis, which appears as a hypoechoic lesion within the tendon as described in more detail previously. Tendinosis should always be carefully differentiated from anisotropy. In particular, the convexity of the insertional footprint of the supraspinatus tendon may mislead sonographers into believing that tendinosis or tearing is present in the areas of hypoechogenicity, when this actually represents anisotropic tendon fibers. Tears in the supraspinatus may also involve other tendons of the rotator cuff. This is particularly the case for the infraspinatus, which intermingles fibers of its insertion toward the lateral edge of the supraspinatus tendon insertion on the middle facet. Tearing of the supraspinatus that extends posterior to the middle facet indicates likely involvement of the infraspinatus tendon. Tearing can also extend anteriorly into the rotator interval, coinciding with pathology of the subscapularis and biceps tendon.

The supraspinatus tendon is the most common rotator cuff tendon affected by calcific disease [30, 31]. The precise pathogenesis of tendon calcifications is unclear, and multiple different etiologies have been proposed [30–32]. Calcific

lesions follow a predictable progression, resulting in the deposition of hydroxyapatite crystals within the tendon [32]. This involves a precalcific stage, where fibrocartilaginous metaplasia occurs within the tendon, followed by the painful formation of hydroxyapatite crystals on these metaplastic tissues that then calcify [32]. This is followed by resorption of the calcific lesion, which may also be painful secondary to increased edema and intratendinous pressure [30]. The pain in both of these stages may be related to ingrowth of neovessels and neonerves [33]. The area of previous calcification is eventually replaced by granulation tissue that is gradually remodeled into normal tendon [30].

On ultrasound, the appearance of these lesions can vary, and several classification systems have been devised to describe them as noted below [34]. While many lesions are hyperechoic with posterior acoustic shadowing, they may also be amorphous in appearance without significant posterior shadowing [34]. They may also take on several different appearances, including arc-shaped, fragmented with multiple components, nodular without shadowing, or cystic with an anechoic center [34]. The consistency of calcifications can also vary from hard, soft, or nearly liquid [35]. Soft or liquid calcifications may be isodense on ultrasound and absent on radiographs, making identification challenging. In these cases, the calcification can be identified as an amorphous echotexture within the tendon that will not become anisotropic with movement of the ultrasound probe [5]. As mentioned earlier, these lesions may also show color and power Doppler signal as a result of closely associated neovessels.

Calcific Disease Classification Systems	
Gärtner and Heyer Classification [36]	
Type I	Dense, well-circumscribed calcification
Type II	Soft contour/dense or sharp/transparent
Type III	Translucent/cloudy, not clearly circumscribed
Molé et al. Classification [37]	
Type A	Sharp contour, dense, homogenous
Type B	Sharp contour, dense, segmented
Type C	Soft contour, heterogeneous
Type D	Dystrophic calcification at the tendon insertion

Interventional Procedures

While corticosteroids are commonly used for shoulder pain, their utility for treatment of tendon injury has been increasingly questioned, given the non-inflammatory etiology of most chronic tendon abnormalities and the potentially harmful impact steroid has on tendon healing [2, 38] Attention has turned to alternative modes of treatment as a result, including platelet-rich plasma (PRP), prolotherapy, and mesenchymal stem cells.

Precise data on treatment of the supraspinatus tendon is muddied by the frequent use of the imprecise term “rotator cuff” in the literature, rather than specifying the tendons being treated. This makes it difficult to evaluate exactly what was targeted in many of these studies and to determine whether one or multiple tendons were addressed with the intervention. Additionally, much of the research has been done within the orthopedic community using platelet-rich plasma as an adjunct to surgical intervention as a way to augment healing outcomes. Several high-quality studies in these cases found borderline effects or failed to show an effect of PRP in these cases [39–43]. Some studies have reported faster healing, decreased retear rates, and lower rates of surgical failure or incomplete healing, but this may be more reliably the case for small to medium tears rather than large or massive tears [41, 44, 45]. The degree to which this reflects an improvement in functional outcomes is also questionable [44, 46]. A Cochrane review found similar findings to this effect [47].

Variable results have been reported for PRP injections as a nonoperative option for treatment of supraspinatus pathology. An RCT comparing PRP to saline injections into interstitial supraspinatus tears found no difference between PRP and saline [48]. At least one study comparing the effectiveness of dry needling with PRP to the supraspinatus tendon found a beneficial effect on pain and disability when PRP was injected into the lesion under ultrasound guidance [49]. Another study by Kesikburun et al. found no difference between PRP and saline, but the injections were placed in the subacromial space rather

than in the tendon [50]. A recent meta-analysis by Lin et al. comparing PRP to steroid and prolotherapy found some indication that PRP improved long-term function more than other therapies and that prolotherapy improved long-term pain more than other therapies [51]. They also noted significant heterogeneity in their data [51]. In particular, the included studies contained a mix of diagnoses including supraspinatus tendinitis, clinically diagnosed subacromial impingement, and chronic tendinosis with 19 studies performing a subacromial injection and only two performing a supraspinatus tendon injection [51]. The effect of PRP composition on effectiveness is an additional consideration that likely influences outcome [52]. This was demonstrated in a 2019 study by Kim et al. that found improved response to PRP injection for degenerative rotator cuff tendinopathy when the injectate had higher levels of IL-1β or TGF-β1 [53]. This level of detail is often not obtained or reported in most PRP studies.

As mentioned above, prolotherapy has been considered for treatment of rotator cuff pathology, both alone and as an adjuvant to other regenerative therapies. However, prolotherapy has received significantly less research attention than PRP. A 2019 meta-analysis of prolotherapy trials for rotator cuff disease found only five randomized-controlled trials and three additional non-randomized trials [10]. While their synthesis of the data showed potential for effectiveness in pain reduction, range of motion improvement, and functional improvement, they also noted significant risk of bias and highly variable findings [10]. This was related to the heterogeneous and often small populations studied, variable sites and methods of injection, differing controls, and differing protocols used. While several studies found positive short-term results with intratendinous injection, long-term follow-up did not show significant differences compared to controls [54–56]. Definitive conclusions about the effectiveness of prolotherapy cannot be made at this time.

Hyaluronic acid has also been proposed as a treatment for rotator cuff tendinopathy, but results of trials to this effect are difficult to interpret, given the variable location of injection. A meta-analysis done by Osti et al. showed effectiveness of hyaluronic acid in treatment of shoulder pain in shoulders with rotator cuff tears; however, the studies included also reported a mix of intra-articular and subacromial locations for injection [57]. A 2019 study by Cai et al. found increased effectiveness of PRP injections when combined with hyaluronic acid injections, when injections were performed in the subacromial space [58]. Of note, research done by Wu et al. examining the effect of intratendinous injections of hyaluronic acid into the Achilles tendon showed a persistent inflammatory response lasting approximately 42 days with a significant increase in neovascularization [59]. These findings led them to recommend against intratendinous injection of hyaluronic acid [59].

While significant enthusiasm has surrounded the use of mesenchymal stem cells (MSC), either derived from adipose tissue or bone marrow, few studies have been performed on the effectiveness of these interventions on tendon pathology of the rotator cuff. Kim et al. evaluated the use of BMAC for rotator cuff pathology compared to an exercise program [60]. They found marginal improvement in pain and function scores at 3 months compared to exercise alone [60]. Jo et al. recently reported an unblinded, uncontrolled case series of adipose-derived MSC injection into rotator cuff tears, although which tendons of the rotator cuff were targeted was not clarified in the study [61]. Those in the high-dose treatment group ($1x10^8$ cells injected) improved in shoulder pain and disability index (SPADI) and visual analogue scale (VAS) with other tested parameters largely nonsignificant (Jo et al. [61]). These studies have yet to be replicated, and caution should be exercised in extrapolating their findings.

Injection Technique

- Patient positioning – Lateral decubitus with affected side facing up
- Transducer selection – High-frequency linear array transducer (>10MHz)
- Transducer position – Long axis to the supraspinatus tendon

- Needle selection – 25–27-gauge 1.5–2.5-inch needle, depending on body habitus and depth of target.
- Injectate selection – Anesthetize with local anesthetic. Inject with ~3 mL of volume including steroid, prolotherapy, or orthobiologic therapy.
- Needle trajectory and target – In-plane, lateral to medial. Target area of tendon pathology.
- Accuracy – Specific studies have not been performed on injections into the supraspinatus, although targeting specific lesions within the tendon without guidance would be extremely challenging. Many studies noted above use injection into the subacromial space with accuracy for these injections reported in the section on the SASD bursa.
- Pearls/Pitfalls
  - It is common to see apparent extension of the lesion under ultrasound guidance as the injectate expands collapsed areas of tearing with the injectate filling these potential spaces.
  - The overall space within an area of pathology may be very limited. Significant pressure should not be exerted during the procedure. Once significant resistance is met, the needle can be withdrawn and redirected to another area of pathology.
  - Some practitioners perform needle tenotomy during injection of PRP to further stimulate inflammation and healing in the area. [62].

Percutaneous needle barbotage/lavage of intratendinous calcific lesions has been found to be a safe and effective means of treating these lesions [63]. However, while short-term results after this procedure appear promising, one long-term follow-up study done by de Witte et al. found no difference in pain, function, or radiographic findings between those who had undergone barbotage and those who had an isolated subacromial corticosteroid injection [64, 65]. They theorize that this may be related to the natural course of calcific lesions, which often resolve on their own [30, 32, 64].

One-Needle Technique

- Patient positioning: Supine with several pillows under the affected shoulder to elevate it
- Transducer selection – High-frequency linear array transducer (>10MHz)
- Transducer position – Long axis to the supraspinatus tendon with the calcification in view
- Needle selection – 16–25-gauge needles have been used, but 18-gauge 2.5-inch needle is recommended
- Injectate selection – Anesthetize down to the lesion. 10mL syringe with 3 mL of 2% lidocaine and 3 mL normal saline attached to the first 10 mL syringe to aid with anesthetizing the lesion. Subsequent syringes can be filled with 6 mL of normal saline.
- Needle trajectory and target – In-plane, lateral to medial. Target calcification.
- Description – Puncture the calcification at a single location if possible. Once the needle is within the calcification, the plunger of the syringe should be gently pumped using back pressure to extract the calcific debris. Calcific debris should be seen returning into the syringe when pressure is released. Once the syringe becomes cloudy, it should be switched for another syringe. This procedure should be repeated until no further calcific debris returns.
- Pearls/pitfalls
  - The needle and syringe should be held in a dependent positioning, so that gravity carries debris away from the needle inlet to avoid reinjection of calcific debris.
  - A single-entry point should be used for best effect. If multiple puncture sites are made, it may not be possible to generate the intralesional back pressure that facilitates the removal of calcific debris.
  - Ensure multiple syringes with normal saline are readily available prior to beginning the procedure, since multiple are commonly required before all calcific debris is removed.
  - If the needle becomes clogged during the procedure, the needle can be withdrawn into the surrounding tissue and then threaded with a 25-gauge needle to clear the blockage.

Two-Needle Technique

- Patient positioning: Same position as above
- Transducer selection – High-frequency linear array transducer (>10MHz)
- Transducer position – Long axis to the supraspinatus tendon with the calcification in view
- Needle selection – 16–25-gauge needles have been used, but 18-gauge 2.5-inch needle is recommended
- Injectate selection – Anesthetize down to the lesion. 6 mL NS attached to 10 mL syringe for calcific tendinosis
- Needle trajectory and target – In-plane, lateral to medial. Target calcification.
- Description – In this technique, two needles are placed within the calcification: one anteriorly that will serve as the injecting needle and one posteriorly in a dependent position that will serve as the draining needle. When both needles have been placed, the syringe is attached to the anterior needle, and the calcification is irrigated with normal saline, which is allowed to drain from the posterior needle. This is done until no further calcific debris drains from the needle.
- Pearls/pitfalls
  - This technique is ideal when back pressure is lost as a result of multiple punctures.
  - If desired, the anterior needle may be repositioned after the procedure to perform a SASD bursa injection.

Subscapularis Tendon

Anatomy and Ultrasound Evaluation

The subscapularis muscle originates in the subscapular fossa on the ventral side of the scapula. It then courses posteromedially to the humerus under the coracoid process to insert anteromedially on the lesser tuberosity of the humerus. The subscapularis lies medial to the biceps tendon over the anterior shoulder and inferior to it in the rotator interval. It serves to internally rotate the shoulder.

The subscapularis is often evaluated after the biceps tendon because of its close proximity. The distal end of the subscapularis tendon is seen in long axis medial to the biceps tendon during short-axis evaluation of the proximal biceps tendon (Fig. 5.2). Positioning the patient in adduction and external rotation brings more the distal tendon into view and allows for Fig. optimization to better evaluate for pathology (Fig. 5.8). Heel-toe movements of the transducer eliminate anisotropy at the footprint of the tendon as it wraps around the humeral head. Full evaluation of the more proximal tendon is limited because of its depth and surrounding bony anatomy. The transducer should be translated superiorly and inferiorly at the lesser tuberosity to ensure that the entirety of the subscapularis tendon is evaluated in long axis.

The transducer is then rotated 90° to evaluate the tendon in short axis. The subscapularis contains several hypoechoic divisions within the tendon in this plane, which represent different tendon bundles and should not be interpreted as partial- or full-thickness tearing of the tendon (Fig. 5.9).

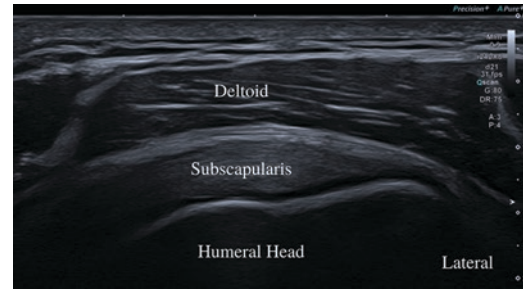

Fig. 5.8 Longitudinal view of the insertional subscapularis onto humerus

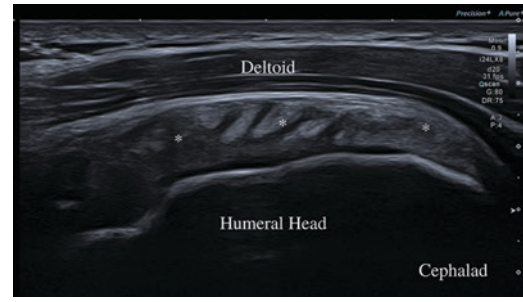

Fig. 5.9 Transverse view of the insertional subscapularis onto humerus. The subscapularis tendon has a unique multipennate appearance

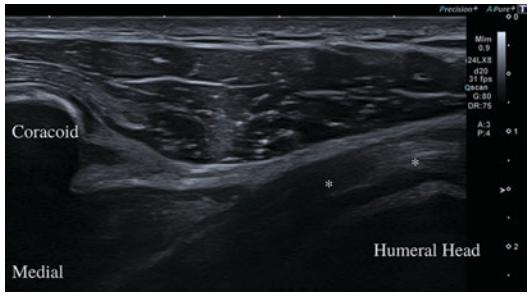

Fig. 5.10 Longitudinal view of subscapularis (*) medially deep to coracoid

Dynamic evaluation is performed to evaluate for subcoracoid impingement medially and bursal fluid that may become more prominent with shoulder internal and external rotation (Fig. 5.10). The subscapularis tendon is visualized in its long axis with the coracoid process visible medially and the humeral head visible laterally. The shoulder is then both passively and actively internally and externally rotated while visualizing the tendon passing under the coracoid process. Any dyskinetic bunching of tissue at the coracoid process, collection of fluid, or pain with this maneuver suggests an underlying pathology.

Pathology

Subscapularis tendon tears commonly occur as a result of acute trauma with the arm abducted and externally rotated and have a similar sonographic appearance as described in the section on the supraspinatus. Isolated subscapularis tears are uncommon and should prompt more thorough evaluation of the rotator cuff [66]. Partial-thickness subscapularis tears can be bursal-sided, interstitial, or articular-sided. The cephalad portion of the tendon is more commonly torn than the caudad portion and is commonly associated with a supraspinatus tear [6, 66].

Full-thickness subscapularis tears can be seen as a discontinuity in the tendon structure or outright retraction if the tear is large or complete. Tears of this nature are most common at the lesser tuberosity and can be seen more clearly in external rotation [5]. Avulsion tears will often demonstrate posterior acoustic shadowing behind the hyperechoic fragment.

It is important to recognize that subscapularis tears are often associated with biceps long head tendon instability, particularly in tearing of the cephalad subscapularis, because of the subscapularis contribution to the rotator interval and stabilizing ligaments that overlie the biceps tendon and constrain medial movement [13].

Subcoracoid impingement occurs as the subscapularis passes deep to the coracoid process. This impingement occurs with internal rotation and shoulder flexion, when the lesser tuberosity of the humerus comes into closest proximity with the coracoid, and can contribute to tendon degeneration, further exacerbating the impingement and increasing tendon thickness [67]. Subcoracoid impingement is much less common than subacromial impingement but may be seen in the settings of postoperative and post-traumatic lesser tuberosity abnormalities [67].

The subcoracoid bursa is located deep to the conjoined tendon of the short head of the biceps and coracobrachialis. It is an extension of the subacromial subdeltoid bursa and does not communicate with the glenohumeral joint. It is commonly enlarged in the setting of anterior rotator cuff pathology [6]. External rotation can draw the bursa out from underneath the coracoid and improve visualization [5]. It should be differentiated from the nearby subscapularis recess. This recess (sometimes known as the subscapularis bursa) is a recess of the glenohumeral joint and overlies the portion of the subscapularis tendon closest to the scapular neck. The recess is typically not visible during routine scanning but may be visible in the setting of an intra-articular effusion. If present, it lies in close proximity to the subscapularis tendon just caudal to the coracoid process [6].

Several studies have attempted to establish defined normal and abnormal coracohumeral distances, but multiple studies have shown mixed results regarding the predictive value of coracohumeral distance [68]. While distance is

unlikely to be indicative in and of itself, abnormal sonographic appearance of the subscapularis tendon combined with abnormal contact under the coracoid in the setting of corresponding anterior shoulder pain is strongly suggestive of impingement.

Interventional Procedures

Data regarding the effectiveness of PRP for treatment of subscapularis pathology suffers from the same lack of specificity in language, target site, intervention protocols, and choice of outcome measures as the supraspinatus literature. In spite of the differences between pathology affecting the subscapularis and supraspinatus, both are often grouped together as rotator cuff pathology with most injections taking place within the subacromial space. As a result, specific data on subscapularis pathology and the effectiveness of PRP, prolotherapy, MSC, or hyaluronic acid is lacking at this time.

- Patient positioning – Supine with arm externally rotated
- Transducer selection – High-frequency linear array transducer (>10 MHz)
- Transducer position – Long axis to the subscapularis tendon
- Needle selection – 25–27-gauge 1.5–2.5-inch needle, depending on body habitus and depth of target. A longer needle is often needed for the subscapularis due to depth of the targeted structures.
- Injectate selection – Anesthetize with local anesthetic. Inject with ~3 mL of volume including steroid, prolotherapy, or orthobiologic therapy.
- Needle trajectory and target – In-plane, lateral to medial. Target area of tendon pathology.
- Accuracy – Studies to have not been performed evaluating the accuracy of these kinds of injections beyond general accuracy of injections into the subacromial space mentioned elsewhere.
- Pearls/pitfalls – None

Infraspinatus

Anatomy and Ultrasound Evaluation

The infraspinatus originates within the scapular infraspinous and courses laterally over the posterior glenohumeral joint to insert on the middle facet of the humoral greater tuberosity. The patient can be examined either seated or side-lying with the shoulder neutrally positioned. The lateral inserting tendon is superficial and should require minimal depth with a superficial focal zone for evaluation. A high-frequency linear probe is usually the best choice for this evaluation. Examination of the medial infraspinatus muscle belly requires greater depth to visualize the entirety of the muscle belly. This should be possible with a linear probe in most individuals but may require a lower frequency curvilinear probe in more muscular or obese individuals.

To identify the infraspinatus, the transducer is aligned in an axial oblique plane inferior to the spine of the scapula. The hyperechoic central tendon can be followed from medial to the lateral insertion of the tendon on the middle facet of the humeral greater tuberosity (Fig. 5.11). The full width of the tendon should be scanned in cephalad to caudad manner, with the most superior aspect of the tendon demarcated by the supraspinatus tendon inserting on the superior and middle facets. It's important not to confuse anisotropy from oblique supraspinatus fibers for infraspinatus pathology.

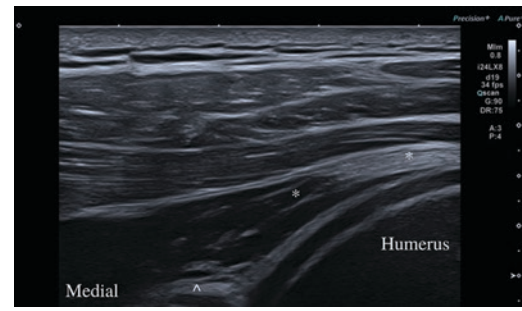

Fig. 5.11 Longitudinal view of infraspinatus (*) overlying the posterior glenohumeral joint. Deep to infraspinatus, the glenoid (^) and humeral head are visualized

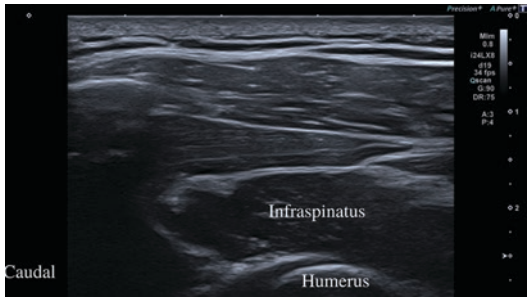

Fig. 5.12 Transverse view of infraspinatus overlying the scapula

Fig. 5.13 Transverse view of infraspinatus (*) overlying the humeral head near its insertion

Toggling or rotating the probe should eliminate these areas of hypoechogenicity.

The infraspinatus should also be evaluated in short axis. The transducer is placed in a sagittal orientation just caudal from the spine of the scapula overlying the infraspinatus in short axis (Fig. 5.12). The musculature and punctate hyperechoic central tendon can be traced from medial to the lateral humeral insertion (Fig. 5.13). The appearance of the muscle belly of the infraspinatus should be compared to the appearance of the supraspinatus teres minor, since changes in muscle echotexture may reflect underlying fatty infiltration from chronic disuse, tearing, or denervation. The use of the panoramic scanning feature can facilitate visualization of the supraspinatus, infraspinatus, and teres minor in one image across the scapula to compare muscle bulk and echotextures.

Pathology

Isolated infraspinatus injury is rare, and tearing often coincides with supraspinatus pathology. Infraspinatus tearing appears similar to supraspinatus tearing as described previously. Full-thickness tears usually indicate concomitant supraspinatus tearing and rarely occur in isolation [5]. Chronic tendon injury can lead to tendinopathy and calcific disease in the infraspinatus through a similar process to that seen in the supraspinatus, although this pathology is less commonly seen [69].

Articular surface tearing of the infraspinatus tendon may also be seen in shoulder internal impingement. This occurs in a position abduction and external rotation of the shoulder [70, 71]. Such tearing is particularly common close to the infraspinatus-supraspinatus junction and may also been seen in conjunction with SLAP tears [70]. These injuries are commonly seen in throwing athletes, and the same torsion forces, shearing, and peel-back forces that result in a SLAP tear are also responsible for articular-sided infraspinatus tears [70]. Chronic microtrauma to the posterior capsule leads to thickening, fibrosis, and subsequent malpositioning of the humerus during abduction and external rotation [70]. Identification of an articular-sided infraspinatus tear should prompt supraspinatus evaluation and a shoulder MRI to assess the labrum.

Interventional Procedures

The evidence for regenerative treatment of the infraspinatus is limited. The vast majority of existing evidence has been done for generic rotator cuff pathology with injection into the subacromial space as described in the section on the supraspinatus. At time of writing, no systematic studies exist examining treatment specifically of the infraspinatus tendon with regenerative therapies. However, given the previously mentioned data on effective treatment regimens for the supraspinatus and rotator cuff, outcomes of similar treatment in the infraspinatus may be similar.

- Patient positioning – Lateral decubitus with affected side facing up
- Transducer selection – High-frequency linear array transducer (>10 MHz) or low-frequency curvilinear transducer (<10 MHz) may be

used for deep targets or to facilitate needle placement
- Transducer position – Long axis to the infraspinatus tendon
- Needle selection – 27-gauge 1.5-inch or 27-gauge 2.5-inch needle, depending on body habitus and depth of target.
- Injectate selection – Anesthetize with local anesthetic. Inject with ~3 mL of volume including steroid, prolotherapy, or orthobiologic therapy.
- Needle trajectory and target – In-plane, lateral to medial. Target area of tendon pathology.
- Accuracy – Studies to have not been performed evaluating the accuracy of these kinds of injections beyond general accuracy of injections into the subacromial space.
- Pearls/pitfalls: None

Teres Minor

Anatomy and Ultrasound Evaluation

The teres minor muscle primarily originates from the axillary border of the scapula caudal to the infraspinatus but also has two aponeurotic laminae that arise from the infraspinatus and teres major muscles. The muscle courses superolaterally to insert onto the humeral greater tuberosity inferior facet and directly on the shaft of the humerus. The teres minor externally rotates and adducts the humerus. It is important to note that the fusion of the infraspinatus and teres minor muscles is a normal variant that may be seen. In this case, the paired muscle bellies share a common aponeurosis that inserts broadly on the greater tuberosity [6].

For ultrasound examination, the patient can be maintained in the same neutral position as the infraspinatus evaluation. The teres minor muscle is identified just caudal from the infraspinatus muscle and has a more rounded appearance in short axis compared to the elongated appearance of the infraspinatus. A subtle ridge in the infraspinatus fossa may also be seen in short axis separating the muscle bellies of each muscle. In long axis, the tendon of the teres minor is very short relative to the infraspinatus and is obliquely oriented relative to the humerus because of its superolateral direction of insertion (Fig. 5.14). The muscle and tendon should be evaluated in short axis from the origin on the scapula to the insertion on the greater tuberosity (Fig. 5.15). While the infraspinatus and teres minor can be differentiated over the scapula, some examiners may find it easier to visualize the tendons over the humerus and trace the tendons back into the musculature to ensure the correct structure is evaluated. In these cases, the teres minor will be the smaller and more inferior tendon seen inserting on the inferior facet.

As previously mentioned, the thickness and echotexture of the teres minor should be evaluated relative to the musculature of the other rotator cuff muscles in the dorsal plane of the scapula. This comparison can be easily achieved for the infraspinatus given the proximity of the muscle

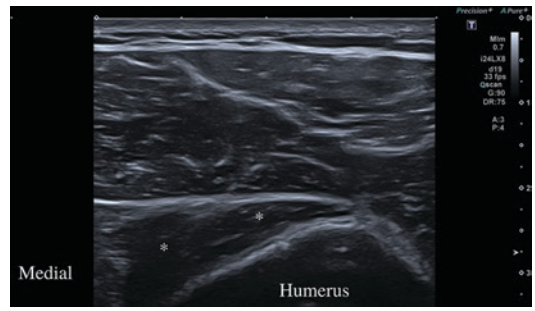

Fig. 5.14 Longitudinal view of teres minor (*) at its humeral insertion

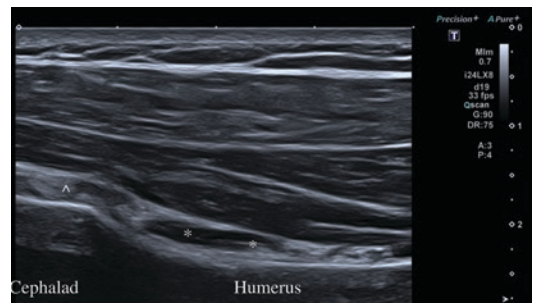

Fig. 5.15 Transverse view of the teres minor (*) at its humeral insertion. Infraspinatus (^) is visualized cephalad/proximal on the humerus from the teres minor

bellies. Comparison between all three muscles requires panoramic evaluation. Since the teres minor is the smallest of the rotator cuff muscles and is rarely injured, it often serves as a helpful reference point for pathology of the supraspinatus and infraspinatus.

Pathology

Teres minor pathology is rare relative to the other muscles of the rotator cuff. Teres minor tendon injury is usually related to acute trauma directly affecting the area. Extension of tears from the infraspinatus tendon into the teres minor tendon is also rare [5]. Signs of denervation may be observed in the teres minor and are commonly caused by impingement of the axillary nerve in the quadrilateral space as discussed elsewhere in this chapter. While the deltoid may be involved, isolated teres minor atrophy can also occur, depending on the exact location where the innervating nerve is entrapped [72]. The innervation of the teres minor has been found to be variable, likely explaining how the teres minor might be selectively affected over other muscles innervated by the axillary nerve [72]. The bundles within the teres minor may even be selectively affected, as noted in a 2019 study by Kang et al. [73].

Interventional Procedures

No systematic studies of regenerative treatment for the teres minor tendon pathology have been performed, likely because the rarity of teres minor pathology, so recommendations beyond those made for the general rotator cuff as discussed in the section on the supraspinatus cannot be made. If quadrilateral space pathology is suspected as a possible cause of denervation of the teres minor, evaluation and injection for this space is discussed in the section on the quadrilateral space. Injections into the teres minor and muscle are rare but follow the same procedural guidelines as those for the infraspinatus.

Subacromial/Subdeltoid Bursa (SASD Bursa)

Anatomy and Ultrasound Evaluation

The SASD bursa is located deep to the acromion, deltoid, and subdeltoid fascia [74] and superficial to the supraspinatus tendon [75, 76]. It averages 55.6 mm medial to lateral length and 55.7 mm in anterior to posterior width. It is a potential space and is very thin when not inflamed, scarred, or distended with fluid [75]. It may extend as far anterior as the acromioclavicular (AC) joint [75]. The SASD bursa does not communicate with the glenohumeral (GH) joint [76], unless a full-thickness rotator cuff tear exists. As it passes around the proximal humerus, the axillary nerve courses about 1.0 cm caudal to the posterolateral boarder of the SASD bursa (range 0.0–1.4 cm) [74, 77].

On ultrasound evaluation of the SASD bursa, the patient's arm in held in adduction and neutral rotation. The probe is oriented in long axis to the supraspinatus tendon in the coronal or coronal-oblique plane with the acromion in view (image of probe placement). A high-frequency linear array transducer is optimal and will be utilized in even the most muscular or obese patients, given the relatively superficial location of the bursa. The SASD is a thin potential space in normal states, appearing as a thin hypoechoic plane overlying the rotator cuff tendons (Fig. 5.16). When acutely or chronically inflamed, the bursa appears as a 2 mm or thicker complex comprised of an

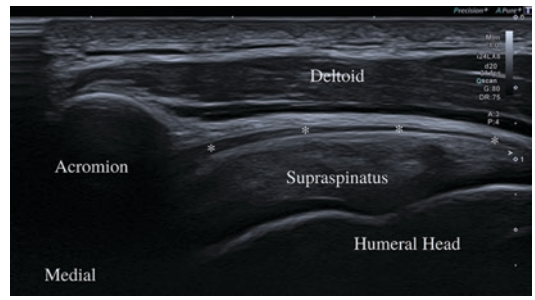

Fig. 5.16 The subacromial-subdeltoid bursa (*) in normal states is visualized as a thin, hypoechoic stripe superficial to the longitudinal supraspinatus and the hyperechoic peribursal fat deep to the overlying deltoid

inner layer of hypoechoic fluid between two layers of hyperechoic peribursal fat [78]. In cases of subtle bursal effusion, fluid accumulates in the most distal and dependent aspect of the bursa and may be visualized several centimeters distal to the insertion of the rotator cuff by sliding the probe laterally [8, 78]. Care should be taken to apply minimal pressure with the probe over the bursa so as to not artifactually displace a bursal effusion.

Pathology

Inflammation of the SASD bursa and pathology involving underlying rotator cuff tendons can lead to bursitis, and subacromial impingement occurs as the enlarged or distended bursa is mechanically traumatized between the rotator cuff tendons and the acromion. Pain related to SASD bursitis or impingement occurs with shoulder abduction, flexion, and internal rotation. SASD bursitis and subacromial impingement are associated with supraspinatus tendon thickening (0.6 mm thicker, $p = 0.048$) that occupation of a greater percentage of the subacromial interval between the acromion and humerus (7.5%, $p = 0.014$) when measured on ultrasound [79]. Dynamic ultrasound can identify dynamic subacromial impingement by passively or actively abducting the arm and evaluating for dyskinetic obstruction of the normal gliding of the SASD bursa under the acromion and pooling of fluid in the distal and lateral SASD bursa [78, 80]. Treatment of SASD bursitis and subacromial impingement consist of physical therapy to improve rotator cuff the glenohumeral stability, relative rest from provoking or exacerbating activities, oral or transdermal non-steroidal anti-inflammatory drugs (NSAIDs), physical modalities (therapeutic ultrasound, manual therapy), interventional procedures (injections), and surgery [81, 82].

Interventional Procedures

SASD bursa corticosteroid injections can successfully palliate symptoms [83]. Only two studies have reported on the injection of orthobiologics into the SASD bursa [84, 85]. Nejati et al. compared two ultrasound-guided injections of leukocyte-rich platelet-rich plasma (PRP) into the SASD bursa and about the rotator cuff tendons (RTC) to a course of physical therapy that progressed from passive range of motion exercises (ROM) to strengthening of the scapular stabilizers. Both interventions effectively reduced pain and disability with the physical therapy cohort showing greater improvement [84]. One study has compared a palpation-guided leukocyte-poor PRP injection to corticosteroid injection and showed that the corticosteroid injection significantly improved pain and function compared to the PRP injection [85]. These studies show that PRP can improve pain, function, and ROM but remain inferior to the more established corticosteroid injections and physical therapy [86].

The accuracy of US-guided SASD bursa injections is 65–100% [87, 88], as compared to 29–100% accuracy of palpation-guided injections [87, 89–92]. A systematic review and meta-analysis comparing US-guided versus palpation-guided SASD bursa corticosteroid injections showed statistically significant differences in pain ($p = 0.003$), function ($p < 0.001$), and range of motion ($p < 0.001$) [83] favoring US guidance.

Procedural protocol:

- Patient position – Lateral decubitus on the contralateral, unaffected side. The arm of the affected side should be adducted, slightly extended, and in slight internal rotation.
- Transducer selection – High-frequency, linear array transducer (>10 MHz).
- Transducer position – Long axis to supraspinatus tendon toward its humeral insertion with the acromion in view. The SASD bursa is identified superficial to the supraspinatus tendon and deep to the deltoid.
- Needle selection – 30-gauge, 1-inch; 27-gauge, 1.5-inch; or 25-gauge, 2-inch (depending on body habitus).
- Injectate selection – Anesthetize with lidocaine or Marcaine. Inject steroid or orthobio-

logic (most commonly PRP). Typically inject 3–5 mL of fluid.
- Needle trajectory and target structure – In-plane, lateral to medial approach to the SASD bursa.
- Pearls/pitfalls
  - Given the convexity of the shoulder, an entry point distal and lateral to the transducer should be chosen to ensure that the needle trajectory is perpendicular to the ultrasound beam.
  - The SASD bursa exists between the deltoid and rotator cuff tendons, which demonstrate differential motion in shoulder internal and external rotation movements and shoulder abduction. Slight movement in those planes can produce differential motion on ultrasound and aid in confirmation of the exact tissue plane of the SASD bursa.
  - A non-distended bursa can be a relatively non-distinct tissue plane, which can make confident identification and accurate injection challenging. Care must be taken to ensure intrabursal flow and not intratendinous or intramuscular deltoid deposition. Accurate intrabursal deposition may accomplish transient retro- or anterograde bursal distension and resolution as the injectate disperses throughout the bursa. Accumulation of fluid in one location without dispersion suggests extrabursal placement [83] and should prompt repositioning of the needle tip.

Acromioclavicular Joint

Anatomy and Ultrasound Evaluation:

The acromioclavicular (AC) joint is a diarthrodial articulation of the acromion and clavicle in the anterolateral shoulder that acts as a strut to anchor the complex movements of the scapula and arm to the thorax [93]. The articular surfaces of the acromion and clavicle are covered with hyaline cartilage. A meniscus-like fibrocartilaginous disc separates those surfaces but has a negligible contribution to joint function [93].

Static stabilizers of the AC joint include the superior, inferior, anterior, and posterior acromioclavicular ligaments, the coracoclavicular ligaments, and the coracoacromial ligaments. The coracoclavicular ligaments reinforce the inferior aspect of the AC joint and prevent superior displacement. Dynamic reinforcement of the joint is provided by the fascia of the overlying deltoid and trapezius muscles.

Ultrasound evolution of the AC joint can be performed with the patient seated or supine. The arm is adducted to the side and shoulder held in neutral rotation. The AC joint is superficial and best evaluated with a high-frequency linear array transducer. Localization of the joint can be facilitated and confirmed by multiple approaches. One reproducible means is to initially place the transducer in an anatomic sagittal plane transversely over the mid-clavicle. The clavicle then appears as a hyperechoic convexity of bone. The transducer is then carefully translated laterally toward the acromion, maintaining the clavicle in this transverse view, until the convex diaphysis of the clavicle flattens and broadens at its epiphysis before falling off into the hypoechoic joint space. The transducer is then maintained at this same position and rotated 90 degrees to longitudinal view of the distal clavicle at its articulation with the acromion (Fig. 5.17).

Normal AC joint space width has been reported in radiographic studies as 1–3 mm at the superior margin of the joint [94]. However, there can be significant variability in joint space measurement because of individual anatomic variations and US probe location. If concern for joint

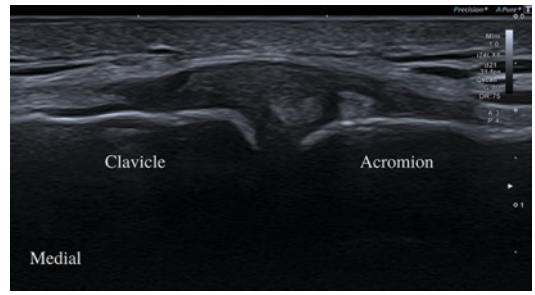

Fig. 5.17 Longitudinal view of the acromioclavicular joint

separation or widening exists, the contralateral AC joint width should be measured and assessed for symmetry. Dynamic evaluation for sonographic widening or narrowing and corresponding pain can be performed by having the patient cross-body adduct their ipsilateral hand to the contralateral shoulder. The acromioclavicular ligament is seen overlying the joint capsule. Other ligamentous stabilizers of the AC joint are obscured from sonographic visualization by surrounding bony anatomy.

The joint can also be evaluated in a long-axis and anatomic sagittal view by scanning along the clavicle in a sagittal oblique plane until the hyperechoic contour of the clavicle rises up superficially before dropping off into the hypoechoic joint space, which contains the hypoechoic fibrocartilaginous disc. This view is rarely used for diagnostic purposes but can be used for in-plane visualization of a needle during an AC joint injection, as described below. The supraspinatus tendon is deep to the AC joint, and a small extent of the tendon can often be visualized through to the joint space.

Pathology

The most common AC joint pathologies are osteoarthritis and ligamentous injury resulting in AC joint separation. AC joint osteoarthritis is characterized by joint space narrowing and cortical irregularities of the clavicle and/or acromion. AC joint degeneration can occur due to age-related degeneration, post-traumatic arthropathy, and, less commonly, distal clavicle osteolysis, inflammatory arthropathy, septic arthritis, and joint instability [95], each of which can contribute to fraying or tearing of the intra-articular disk and maceration of the chondral surface of the diarthrodial joint [96]. Patients with AC joint arthritis will have tenderness with palpation directly over the AC joint and pain with cross-body shoulder adduction [97]. AC joint arthritis is treated conservatively with physical therapy focused on ROM and strengthening of the peri-capsular musculature (which is often ineffective), activity modification, NSAIDs, and intra-articular joint injection [95].

Acromioclavicular joint separation can occur secondary to a traumatic ligamentous sprain or chronic, attritional ligamentous disruption of one or several of the static stabilizers of the joint. The Rockwood classification system is the most commonly used system to classify injuries but is based on radiographic findings from bilateral anterior-to-posterior, axillary, and Zanca views. US correlates to the Rockwood classification are described in Table 5.1. Joint widening, superior clavicular displacement, and increased joint mobility can be identified by ultrasound evaluation; however, many ligaments that stabilize the AC joint cannot be directly visualized with ultrasound, and US measurements of displacement can be inconsistent, both of which can limit its diagnostic sensitivity in the context of suspected separation. AC joint effusion is identified as a hypoechoic, compressible fluid collection that superiorly distends in the joint space greater than 3 mm, and may result from acute injury, chronic degenerative changes, or communicating from the glenohumeral joint in the context of a full-thickness supraspinatus tear [98]. Treatment of AC joint separation depends on the type; anesthetic injections can be performed for pain control.

An os acromiale results from incomplete fusion of the anterior epiphysis of the acromion and is present in about 8% of the population and is present bilaterally in about one third of that population [100]. The os acromiale can relate to the lateral acromion by means of a separate articulation, a fibrocartilaginous union, or nearly complete fusion [100]. Pain can result from anterosuperior impingement of the underlying subscapularis tendon by a mobile os body or by secondary osteophytes. This synchondrosis should not be mistaken for a fracture or for the true AC joint. The acromion's articulation with the os acromiale can be differentiated from the true acromioclavicular joint by its orientation, which is approximately perpendicular to the plane of the acromioclavicular joint [6, 101].

Table 5.1 AC joint separation Rockwood classification with ultrasound correlation

Type	Definition		Radiographs	US description
	AC ligament	CC ligament		
1	Sprain	Normal	Normal	Asymmetric joint space widening. Irregular-appearing capsular fibers. Hypoechogenic edema within the joint space. No step off between the clavicle and acromion
2	Torn	Sprain	Superiorly displaced lateral clavicle. Increased coracoclavicular distance <25%	Visible step off between the (medial) clavicle and (lateral) acromion. Joint space widening and increased clavicle mobility when stressed
3	Torn	Torn	Superiorly displaced lateral clavicle. Increased coracoclavicular distance 25–100%	More prominent step off between the clavicle and acromion. Joint space widening and increased clavicle mobility when stressed
4	Torn	Torn	Posteriorly displaced lateral clavicle	Horizontal instability with dynamic maneuvers with posterior clavicular displacement [99]
5	Torn	Torn	Superiorly displaced lateral clavicle. Increased coracoclavicular distance >100%	Acromioclavicular step off greater than 100%. Joint space widening when stressed
6	Torn	Torn	Inferiorly displaced lateral clavicle	There is a larger step off between the acromion and clavicle with the clavicle displaced inferiorly

An AC joint cyst results from glenohumeral joint fluid tracking into the acromioclavicular joint because of a massive rotator cuff tear, leading to significant distension of the superior joint capsule. On coronal evaluation of the AC joint, this can appear as hypoechoic fluid emerging from the underlying narrow joint space and termed a "geyser sign." This finding should prompt a full evaluation of the rotator cuff.

Interventional Procedures

AC joint anesthetic injection can be performed for diagnostic purposes in the context of AC joint arthritis or cysts to assist the clinic decision-making [102–104] and for analgesia in the setting of AC joint separation [105]. AC joint corticosteroid injections have been reported to have poor efficacy in symptom palliation and to achieve only short-term benefit [103, 106]. Definitive management can include surgical resection of the distal clavicle, but this can result in postoperative joint instability [95, 103, 106, 107]. Orthobiologics can be used to treat AC joint pathology, but only one study on prolotherapy has been reported. That study describes the use of ultrasound-guided injection of 15% dextrose prolotherapy into the AC joint (one or two injections 1 month apart) or near the distal acromion and showed substantial pain reduction with average visual analog scale (VAS) reduction of 4.3 points ($p < 0.01$) [108].

Despite the superficial location of the AC joint, accuracy of palpation-guided AC joint injections is very low (36.5–72%) [91, 109–112]. Ultrasound-guided injections of various approaches have accuracies of 90–100% but have not been directly compared [109, 110].

Procedural protocol: AC joint injection, anterior to posterior

- Patient position – Supine or seated. The ipsilateral shoulder and arm are held at the side in comfortable, neutral anatomic positions.
- Transducer selection – High-frequency, small-footprint linear array transducer (>10MHz). The small footprint aids in maneuverability of the probe and needle.
- Needle selection – 30-gauge, 1-inch; or 27-gauge, 1.5-inch.
- Injectate selection – Local anesthesia is often not used since the joint is so superficial. Inject anesthetic (for diagnostic purposes), steroid,

orthobiologic (PRP or prolotherapy). Typically inject <1 mL of fluid.

- Technique #1.
  - Transducer position – Short axis to clavicle over joint with no bony structures in view. Anatomic sagittal plane. The hypoechoic AC joint space is identified between the hypoechoic margins of the clavicle and acromion.
  - Needle trajectory and target – In-plane, anterior to posterior into AC joint.
  - Pearls/pitfalls

    The AC joint is very small; therefore, only the smallest volume as needed should be injected, usually about 1 mL.

    The location of the needle insertion site at the skin should take into account the convexity of the anterior shoulder and the depth of the joint space from the skin and the joint capsule to facilitate a near-parallel trajectory to the joint for optimal needle visualization.

    The transducer can be rotated 90 degrees to confirm that the needle tip is in the joint in an out-of-plane visualization between the clavicle and acromion.
- Technique #2
  - Transducer position – Long axis to clavicle and acromion with those bony contributions to the joint completely visualized. Anatomic axial plane. The hypoechoic AC joint space is identified between the hyperechoic convex margins of the clavicle and acromion.
  - Needle trajectory and target – Out-of-plane, anterior to posterior into the AC joint.
  - In an out-of-plane approach, the needle is visualized as a hyperechoic, punctate dot. The ultrasound transducer should be translated anteriorly (toward the sternum) to meet the needle tip shortly after it is inserted into the skin to identify its location and to estimate it's trajectory. Small-caliber translations anteriorly and posteriorly will aid in the triangulation of the superficial/deep and medial/lateral trajectory of the needle to inform whether withdrawal and redirection is necessary to ensure its continued accurate trajectory and its final location within the joint space.

    Pearls/pitfalls
    - Utilizing the walk-down technique is helpful in executing the injection.
    - The AC joint is very small; therefore, a small amount of fluid should be injected.
    - The transducer can be rotated 90 degrees to determine the anterior-posterior location of the needle tip within the joint.
- Technique #3: Lateral to medial AC joint injection
  - Patient position – Supine or seated. The ipsilateral shoulder and arm are held at the side in comfortable, neutral anatomic positions.
  - Transducer selection – High-frequency, small-footprint linear array transducer (>10 MHz).
  - Transducer position – Long axis to clavicle and acromion with those bony contributions to the joint completely visualized. Anatomic axial plane. The hypoechoic AC joint space is identified between the hyperechoic convex margins of the clavicle and acromion.
  - Needle selection – 30-gauge, 1-inch; or 27-gauge, 1.5-inch.
  - Injectate selection – Injection of local anesthesia with lidocaine or Marcaine, as the subcutaneous needle course is slightly longer than anterior-to-posterior approaches. Inject anesthetic (for diagnostic purposes), steroid, or orthobiologic (PRP or prolotherapy) to the joint. Typically inject about 1 mL of fluid.
  - Needle trajectory and target – In-plane, lateral to medial into AC joint.

    A generous gel standoff at the lateral aspect of the transducer overlying the acromion will facilitate an improved needle visualization, as there is often only a

small amount of tissue overlying the acromion and AC joint. A gel standoff permits needle visualization and redirection before skin entry to optimize the approach to the joint and improve ultimate accuracy of needle placement. A skin entry that is too far lateral may dictate an approach trajectory that is too far media or lateral and can make entry into the joint unnecessarily challenging or impossible.

Sternoclavicular (SC) Joint

Anatomy and Ultrasound Evaluation

The SC joint is a saddle-shaped joint between the manubrium of the sternum and first rib medially and the medial end of the clavicle laterally [113]. It is the only articulation between the thorax and the upper limb. The SC joint is stabilized by the anterior and posterior sternoclavicular ligaments, the interclavicular ligaments, and the costoclavicular ligaments [113, 114]. A fibrocartilaginous disk separates the joint into clavicular and sternal compartments. Age-related degeneration can result in communication between these compartments [114, 115].

The sternoclavicular joint is visualized sonogramphically with the probe in a coronal or axial plane spanning the joint, with the clavicle visualized in long axis, and the sternum visualized medially (Fig. 5.18). A small-footprint linear array transducer is most commonly used and should be scanned in a cephalad to caudad maneuver to evaluate the entire joint.

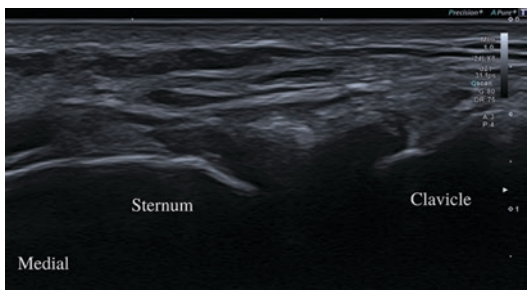

Fig. 5.18 Longitudinal view of the sternoclavicular joint

Pathology

Injuries of the SC joint are uncommon, but acute injuries can be severe to life-threatening. Ultrasound can identify subluxation or dislocation of the SC joint as an excessive, asymmetric step off between the sternum and clavicle. Comparison to the contralateral side is helpful. US can also identify atraumatic pathology, most commonly arthritis. SC joint arthritis occurs most commonly in patients with rheumatoid arthritis; is characterized by narrowing of the joint space, osteophytes, and para-articular cysts; and is amenable to corticosteroid injections. Septic arthritis is associated with increased joint fluid of mixed echogenicity and often requires aspiration and analysis of joint fluid or surgical washout [116].

Interventional Procedures

Description of the use of orthobiologics to treat the SC joint is scarce in the literature. One case reports the use of orthobiologics in the treatment of SC joint instability and describes the use of six injections of prolotherapy (a mixture of 22% dextrose and procaine was used for some injections and "more traditional" prolotherapy for others) and one leukocyte-poor PRP injection, followed by seven additional prolotherapy injections (22% dextrose and 1 mL of sodium morrhuate and procaine) into the bilateral SC joint capsular and ligamentous tissue that resulted in resolution of pain and popping symptoms [117].

The SC joint is not commonly injected, and different methods of guidance have been reported. Palpation-guided injections of the SC joint have a reported accuracy of 78%. Computed tomography (67% accuracy) [118, 119] and fluoroscopy [120] have been successfully used for needle guidance into the SC joint. Sonographic guidance is reported to have a 100% accuracy for injection of the SC joint [121].

Procedural protocol:

- Patient position – Supine or seated. The arm of the affected side is in neutral anatomic position.

- Transducer selection – High-frequency, small-footprint linear array transducer (>10 MHz).
- Transducer position – Spanning the SC joint with the clavicle in long axis.
- Needle selection – 30-gauge 1-inch; or 27-gauge 1.5-inch.
- Injectate selection – Can anesthetize with lidocaine or Marcaine. Inject anesthetic (for diagnostic purposes), steroid, or orthobiologic (PRP or prolotherapy). Typically inject <1 mL of fluid.
- Needle trajectory and target – Out-of-plane, anterior to posterior into the SC joint.
- Pearls/pitfalls.
  - A hyperechoic intra-articular disk may be visualized within the joint.
  - Take caution to avoid advancement of the needle beyond the SCJ where it can injure neurovasculature.
  - The transducer can be rotated 90 degrees to confirm that the needle tip is in the joint.

This injection can also be performed with the same setup using an in-plane, lateral to medial technique with gel standoff. This involves a lateral gel standoff and toe-ing in the medial side of the transducer. The smaller footprint and greater maneuverability of a small-footprint linear array transducer makes this easier. Such an approach, standoff, and small-footprint transducer improve the ease of injection, given the minimal subcutaneous tissue in this area through which to guide or redirect a needle to ensure placement within the joint space.

Glenohumeral (GH) Joint and Rotator Interval

Anatomy and Ultrasound Evaluation

The GH joint is a shallow ball and socket joint comprised of the articulation between the pear-shaped glenoid fossa of the scapula and the spheroidal humeral head. The shallow nature of this articulation affords the most range of motion of any joint in the body. The glenoid labrum is a fibrocartilaginous tissue that encircles the glenoid to extend the depth of the glenoid socket by 50%. The lax and redundant glenohumeral joint capsule allows for a wide range of motion and extends from the margins of the glenoid rim and labrum to the anatomic neck of the humerus. The capsule has several recesses in which fluid can accumulate in the setting of effusion (dependent axillary pouch, posterior and anterior recesses, subscapularis recess, sheath of the long head of the biceps tendon).

The joint is stabilized by both static and dynamic stabilizers. The glenohumeral ligaments provide static stability to the joint (Table 5.2). The glenoid labrum is composed of a fibrocartilaginous tissue and additionally contributes to

Table 5.2 Static stabilizers of the glenohumeral joint

Ligament	Biomechanics
Superior glenohumeral Ligament	Restraint to anteroinferior translation of long head of biceps (biceps pulley) and inferior translation at 0 degrees of abduction
Middle glenohumeral Ligament	Resists anterior and posterior translation in the midrange of abduction (~45 degrees of external rotation)
Inferior glenohumeral Ligament (Posterior Band)	Most important restraint to posterior subluxation at 90 degrees of flexion and internal rotation Tightness is linked to SLAP lesions
Inferior glenohumeral Ligament (Anterior Band)	Primary restraint to anterior/inferior translation 90 degrees abduction and maximal external rotation Weak link predisposing to Bankart lesions
Inferior glenohumeral Ligament (superior band)	Most important stabilizer of the joint
Coracohumeral ligament	From coracoid to rotator cable Limits posterior translation with should in flexion, adduction, and internal rotation Limits inferior translation in external rotation and adducted position Thickened in adhesive capsulitis

SGHL superior glenohumeral ligament, *MGHL* middle glenohumeral ligament, *IGHL* inferior glenohumeral ligament, *SLAP* superior labrum from anterior to posterior

static stability by helping to create 50% of the glenoid socket depth. The anterior labrum anchors the inferior glenohumeral ligament, and the superior labrum anchors the biceps tendon. Several normal variants of the glenoid labrum occur and must not be mistaken for pathology, including a cord-like middle glenohumeral ligament (MGHL), sublabral foramen, sublabral foramen plus cord-like MGHL, and a Buford complex, which consists of an absent anterosuperior labrum and cord-like MGHL. Dynamic stabilizers consist of the periscapular muscles, biceps tendon, rotator interval, and rotator cuff muscles (supraspinatus, infraspinatus, teres minor, subscapularis). The rotator cuff muscles provide dynamic stability by compressing the humeral head against the glenoid.

At the rotator interval, the capsule is reinforced externally by the coracohumeral ligament (CHL) and internally by the superior glenohumeral ligament (SGHL) and traversed by the intra-articular portion of the long head of the biceps tendon [13]. The interval lies between the anterior margin of the supraspinatus and superior margin of the subscapularis tendon [13]. The intra-articular portion of the biceps tendon and the biceps pulley system lie within the rotator interval [13].

On ultrasound evaluation, the posterior GH joint is evaluated using a liner array transducer with the patient seated and the shoulder in neutral rotation. A lower frequency curvilinear array transducer may be necessary in patients with a large or more muscular body habitus. The transducer is placed in an oblique axial plane with the lateral end of the probe angled superiorly toward the humeral head just inferior to the scapular spine. The GH joint is visualized deep to the central tendon of the infraspinatus (Fig. 5.19). The articulation between the humeral head and glenoid should be evaluated from proximally under the acromion to distally to the humeral surgical neck. The posterior glenoid labrum can also be visualized and can be made more conspicuous with shoulder internal and external rotation.

The anterior GH joint and rotator interval are evaluated with the patient in a modified Crass position and the transducer in short axis to the proximal long head of the biceps tendon. The SGHL is located at the subscapularis side of the biceps brachii tendon with fibers merging with the CHL that lies superficial to the biceps tendon. The supraspinatus tendon lies posterolateral to the biceps tendon at the rotator interval, and the hypoechoic ligament, which separates them, should not be misinterpreted as a tendon tear [122]. (Fig. 5.2).

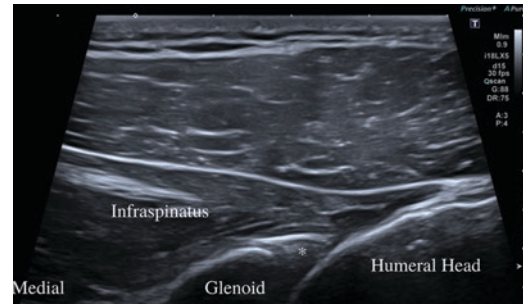

Fig. 5.19 Posterior glenohumeral joint. The posterior articulation the humeral head laterally with the glenoid, medially. The infraspinatus is visualized superficial to the joint space, and the glenoid labrum (*) is visualized as a hyperechoic triangular-appearing structure contiguous with the glenoid

Pathology

A glenoid labral tear can occur secondary to trauma or repetitive microtrauma of overhead activities (SLAP). A labral tear is described by its location and can occur concomitantly with internal impingement, glenohumeral internal rotation deficit (GIRD), rotator cuff tears, and scapular dyskinesis. Ultrasound can be a highly specific tool to identify a posterior labral tear (98%), although it is not highly sensitive (63%) [123]. There is a substantial agreement between sonoarthrography and MR arthrography for the diagnosis of posterior labral tears [124]. Glenohumeral joint injection can be both diagnostic (using anesthetic) and therapeutic for labral injuries [125].

Ultrasound can be applied to accurately evaluate the shoulder after an acute dislocation or subluxation and has been shown to have 100% accuracy in several studies in identifying

the characteristic hypoechoic or anechoic interval between the humeral head and the glenoid [126, 127]. Ultrasound can also identify a Hill-Sachs lesion and dynamically visualize engagement of the humeral lesion within the glenoid rim, an indication for surgical evaluation [128].

GH joint arthritis affects up to 32.8% of those over 60 years old and can develop after shoulder trauma, in the setting of rotator cuff degeneration, or secondary to rheumatoid arthritis [129]. Findings on ultrasound can include marginal osteophyte formation and joint space narrowing. Nonsurgical management of GH osteoarthritis includes activity moderation and modification, NSAIDs, injection therapies, and physical therapy (PT) focused on periscapular strengthening and stretching [130, 131] (1, 12. Surgical interventions can consist of debridement and capsular release, or a type of shoulder replacement) [131–133].

Adhesive capsulitis is characterized by limited range of motion (ROM) followed by shoulder pain. Shoulder external rotation is most commonly affected. It can be idiopathic or can be associated with diabetes mellitus, trauma, and immobilization. It is characterized by three clinical stages (Table 5.3). The most sensitive and specific ultrasound finding reported is a diminished sliding movement of the supraspinatus tendon beneath the acromion with shoulder abduction, which has a 91% sensitivity, 100% specificity, and 92% accuracy for detecting adhesive capsulitis [134]. Abnormal hypoechogenicity and hyperemia at the rotator interval have been demonstrated in up to 86% of patients with adhesive capsulitis [135]. Thickening of the coracohumeral ligament (3 mm vs 1.39 mm in controls) is also seen [136].

Table 5.3 Clinical stages of adhesive capsulitis

Clinical stage	Description
Freezing/ Painful	Gradual onset of diffuse pain (6 weeks–9 months)
Frozen/Stiff	Decreased ROM affecting activities of daily living (4–9 months or more)
Thawing	Gradual return of motion (5–26 months)

Nonsurgical management of GH adhesive capsulitis can include PT, extracorporeal shock wave therapy, corticosteroid injections, and capsular hydrodistension. Most patients will see complete resolution of pain and full return of glenohumeral motion after conservative treatment and time [137–142]. Manipulation under anesthesia or arthroscopic capsular release can be considered in refractory cases [137].

Interventional Procedures

In patients with GH joint arthritis, injection of HA has had shown mixed outcomes. Several small retrospective case series [143–147] and one retrospective case-control study [148] reported a significant reduction in pain and improvement in function in patients with GH arthritis treated with HA, but two large randomized controlled trial did not show superiority of HA to placebo [149, 150]. The majority of the studies utilized palpation guidance for the injections, which may confound the results [144, 146–150]. Only one study reports the injection of PRP into the GH joint, and this was in the context of GH adhesive capsulitis. Cell-based therapies have limited evidence in treating patients with GH joint arthritis. One case series of 115 patients with GH joint arthritis with or without RTC tear showed improved pain and physical function for up to 2 years following bone marrow aspirate concentrate (BMAC) injection, but the study was limited by heterogeneity in the patient population and lack of a control group [151]. A case series of the use of microfragmented adipose tissue (MFAT) to treat 20 patients with GH arthritis and concomitant rotator cuff tear resulted in improvements in pain and function at 12 months [152].

Although orthobiologic injections into the GH joint are sometimes implemented to treat glenoid labral pathology, there are no PubMed indexed studies describing or supporting PRP injections to treat labral pathologies [153].

Ultrasound-guided interventional procedures are commonly performed to treat GH adhesive capsulitis. Corticosteroid injections are generally accepted as a mainstay of treatment with short-

term efficacy, although a high degree of variance is seen in the dose of corticosteroid administered, location of injection, and performance of concomitant procedures at the time of steroid injection [154–159]. Several studies have compared the clinical efficacy of anterior (rotator interval) to posterior GH joint injections in patients with frozen shoulder with two studies showing no clinical difference [160, 161] and one showing faster and more significant improvement with steroid injection into the rotator interval [162]. Hydrodistension of the joint capsule with a high volume of injectate is commonly used to treat adhesive capsulitis, but one meta-analysis of 12 studies reported that it had only a small, clinically insignificant effect [140]. The use of orthobiologics to treat adhesive capsulitis is emerging, with one study demonstrating that injection of a single dose of intra-articular PRP was more effective than intra-articular corticosteroid injection on improving pain, function, and ROM [163] and was more effective than procaine on pain and function [164]. Some advocate for the use of orthobiologics rather than corticosteroids to treat adhesive capsulitis in diabetics to minimize blood sugar elevation, but this has not been specifically reported in the literature.

The use of ultrasound guidance greatly improves the accuracy of GH joint injections relative to palpation-guided injections. Palpation-guided anterior GH joint injections are 26–95.7% accurate [165, 166] and posterior GH joint injections 42–96% accurate [92, 167–169]. Ultrasound guidance of injections to the GH joint improves accuracy to 92% with an anterior approach (rotator interval) [170] and to 92.5–100% with a posterior approach [168, 170–173].

Procedural protocol: Posterior approach to GH joint

- Patient position – Lateral decubitus with the affected side up. The arm should be in neutral or slight internal rotation.
- Transducer selection – Low-frequency, curvilinear (>10 MHz), or midrange linear array transducer
- Transducer position – Short axis to the joint in the oblique axial plane. The transducer should be placed just lateral to the inferior scapular spine.
- Needle selection – 25-gauge, 2.5-inch (or longer if larger body habitus)
- Injectate selection – Anesthetize with lidocaine or Marcaine. Inject steroid or orthobiologic (most commonly PRP). Typically inject 3–5 mL of fluid or > 10 mL if treating adhesive capsulitis.
- Needle trajectory and target structure – In-plane, lateral to medial approach into to the GH joint. Needle will traverse through the infraspinatus musculotendinous unit. Greater glenohumeral internal rotation and cross-body adduction will pull the infraspinatus tendon anteriorly, ensuring that the needle traverses more through musculature than tendon. Ensure that the needle tip is deep to the infraspinatus and glenoid labrum, adjacent to the hypoechoic articular cartilage of the humeral head
- Pearls/pitfalls
  - Take care to identify to not to injure the glenoid labrum.
  - The injectate should flow readily into the large, accommodating GH joint. Visible accumulation of injectate in one area suggests extraarticular placement and should prompt redirection of the needle tip.
  - Placement of the needle superficial and medial to the GH joint poses risk of injury to neurovascular structures in spinoglenoid notch.

Procedural protocol: Anterior approach to GH joint at rotator interval

- Patient position – Supine. The arm adducted and in slight GH external rotation.
- Transducer selection – High-frequency linear array transducer (>10MHz)
- Transducer position – Anatomic axial plane over the rotator interval with the long head of the biceps tendon in short axis.
- Needle selection – 27-gauge 1.5-inch; or 25-gauge 2.5-inch
- Injectate selection – Anesthetic with lidocaine or Marcaine. Inject steroid or orthobiologic.

Volume of about 5 mL, or > 10 mL if treating adhesive capsulitis.
- Needle trajectory and target – In-plane, lateral to medial approach into the space deep to the coracohumeral ligament and superficial to the LHBT.
- Pearls/pitfalls.
  - Slight external rotation of the arm improves visualization of the long head of the biceps tendon and structures of the rotator interval.

Spinoglenoid Notch

Anatomy and Ultrasound Evaluation

The spinoglenoid notch is formed between the lateral side of the scapular spine and the posterior part of the glenoid, and the spinoglenoid ligament spans these two bony structures of the scapula [174]. The suprascapular nerve traverses the spinoglenoid notch before innervating infraspinatus. The suprascapular artery and vein course lateral to the suprascapular nerve in the spinoglenoid notch and occupy 68.5% of the suprascapular notch [175].

During sonographic evaluation, the spinoglenoid notch is localized medial to the posterior GH joint by translating the transducer medial and from the joint and rotating the medial end of the transducer slightly cephalad (Fig. 5.20). Color doppler should be applied to identify the vascular structures within the spinoglenoid notch. Dynamic engorgement of the vein when the arm is in external rotation should not be mistaken for a spinoglenoid notch cyst.

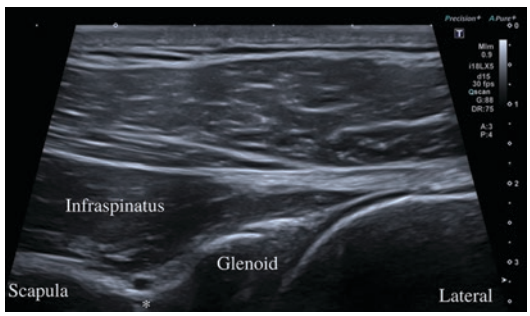

Fig. 5.20 The spinoglenoid notch (*) is visualized between the scapular spine medially and the glenoid laterally. The suprascapular nerve lies within the spinoglenoid notch and infraspinatus superficial to that nerve

Pathology

Compression of the suprascapular nerve in the spinoglenoid notch results in infraspinatus denervation. Neural injury can be secondary to a spinoglenoid notch ganglion cyst [176, 177], GH paralabral cyst secondary to posteroinferior glenoid labral tear (most common) [178, 179], or traction injury, as seen in volleyball players [180]. Cysts can be difficult to visualize on ultrasound due to their deep location. Placing the ipsilateral hand on the contralateral shoulder may make spinoglenoid notch more superficial and improve diagnostic assessment. Paralabral cysts are most commonly visualized in the superficial region of the spinoglenoid notch. If denervation has occurred, the infraspinatus muscle will appear atrophied and hyperechoic relative to the ipsilateral supraspinatus and to the contralateral infraspinatus. The volume of a paralabral cyst has been shown to directly correlate with the degree of infraspinatus atrophy [179]. Infraspinatus denervation can be confirmed with electrodiagnostic studies. Varicosities and enlarged spinoglenoid notch veins are also seen at the spinoglenoid notch. Veins are not stationary and will dynamically vary in size with different shoulder movements. Color Doppler should be used to rule out the presence of blood flow in any cystic-appearing structure.

Interventional Procedures

A sonographically lateral-to-medial spinoglenoid notch paralabral cyst aspiration can have up to an 86% success rate for pain reduction [181]. The use of orthobiologics to treat pathology of the spinoglenoid notch region has not been reported.

Procedural protocol: Spinoglenoid notch injection or cyst aspiration

- Patient position – Lateral decubitus with the affected side up. The arm should be in neutral or slight internal rotation.
- Transducer selection – Low-frequency, curvilinear (>10 MHz)
- Transducer position – Just inferior and parallel to the lateral edge of the spine of the scapula. The medial end of the transducer should be rotated slightly cephalad to optimize visualization of the spinoglenoid notch.
- Needle selection – 27-gauge, 1.5-inch; 25-gauge, 2.5-inch (or longer if larger body habitus) needle can be used for local anesthetic. An 18-gauge 2.5- or 3.5-inch needle should be used for aspiration of a cyst.
- Injectate selection – Anesthetize with lidocaine or Marcaine. Inject steroid or orthobiologic (most commonly PRP). Typically inject 3–5 mL.
- Needle trajectory and target structure – In-plane, medial to lateral approach to the spinoglenoid notch cyst.
- Pearls/pitfalls
  - Color Doppler should be used to rule out the presence of blood flow in any cystic-appearing structure to ensure that the targeted structure is not vasculature.
  - If one wishes to both aspirate/inject in the spinoglenoid notch and to inject into the posterior GH joint, the same needle entry point can be used by slightly withdrawing the needle from the spinoglenoid notch and redirecting the needle more steeply to the more lateral GH joint.

Suprascapular Notch

Anatomy and Ultrasound Evaluation

The suprascapular notch is a U- or V-shaped notch in the lateral body scapula within the supraspinous fossa, which is located just medial to the base of the coracoid and about 3 cm medial from the supraglenoid tubercle [182]. Table 5.4 details the six different anatomical classifications of the notch character [183]. The superior transverse scapular ligament traverses superficial to the notch and forms a roof to a foramen through which through suprascapular nerve travels. The suprascapular artery travels superficial to the ligament [183].

Table 5.4 Suprascapular notch anatomy

Type	Rate of occurrence	Description
1	6–22%	Notch is absent. The superior border forms a wide depression from the medial angle to the coracoid process
2	8–31%	Notch is a blunted V-shaped occupying the middle third of the superior boarder
3	29–60%	Notch is U-shaped with nearly parallel margins
4	3–13%	Notch is V-shaped and very small
5	6–18%	Notch is minimal and U-shaped with a partially ossified ligament
6	2–6%	Notch is a foramen since the ligament is completely ossified

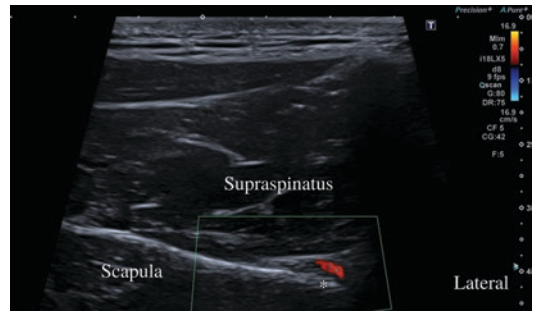

Fig. 5.21 Longitudinal view of the suprascapular notch (*)

Ultrasound evaluation of the suprascapular notch is performed using a curvilinear array transducer with the patient in the seated position. The transducer is placed in long axis to the supraspinatus tendon within the supraspinous fossa just cephalad to the scapular spine. The transducer is angled in a caudad direction and oriented almost directly in a coronal plane, which facilitates visualization of the notch (Fig. 5.21). Depth and focus should be adjusted to optimize the image of the deep suprascapular notch as the muscular bulk of lateral trapezius and supraspinatus can vary greatly between individuals [184].

Pathology

Compression of the suprascapular nerve at the suprascapular notch can occur secondary to a glenohumeral paralabral cyst, a space-occupying lesion, or a massive supraspinatus tear or from repetitive traction related to overhead sports [185]. The notch type (V-shaped is more commonly associated with pathology) and distance from the glenoid may be correlated with injury risk [186, 187]. Pathologic compression can result in infraspinatus atrophy and possibly supraspinatus atrophy, and patients may complain of shoulder pain, demonstrate arm abduction and external rotation weakness, and maintain intact sensation. Ultrasound evaluation should assess for supraspinatus and infraspinatus atrophy, manifested as muscular hyperechogenicity relative to adjacent or superficial musculature and loss of muscular bulk. A paralabral cyst or other space-occupying lesion may be visualized within or adjacent to the suprascapular notch as a rounded or oval hypoechoic lesion with well-defined margins that remains relatively fixed with dynamic shoulder movements [184].

Interventional Procedures

The suprascapular nerve provides sensation to the posterior GH joint and can be blocked prior to surgical procedures or in the setting of severe GH joint pathology not amenable to surgery. The accuracy of ultrasound-guided suprascapular notch injections for suprascapular neural blockade has been reported to be 100% in one cadaveric study [188]. However, another study utilizing EMG current intensity reported that only 18.5% of suprascapular nerve injections were believed to be close enough to the nerve; however, it could be reasonably postulated that the spread of anesthetic injectate or other medication could still result in a sufficient neural blockade [189]. Other studies have shown no difference between ultrasound-guided and landmark-guided suprascapular nerve blocks [190, 191]. There are no reports of the injection of orthobiologics agents near the suprascapular notch.

Procedural protocol: Suprascapular nerve block at the suprascapular notch

- Patient position – Seated with ipsilateral hand placed on contralateral shoulder.
- Transducer selection – Low-frequency, curvilinear (<10 MHz)
- Transducer position – Parallel to the spine of the scapula over the supraspinatus fossa with US beam angled caudally to visualize the suprascapular notch.
- Needle selection – 25-gauge, 3.5-inch needle
- Injectate selection – Anesthetize with lidocaine or Marcaine. Inject anesthetic or steroid. Typically inject 3–5 mL.
- Needle trajectory and target – In-plane, medial to lateral (preferred) adjacent to the suprascapular nerve within the suprascapular notch and deep to the superior transverse scapular ligament. Injection can also be performed lateral to medial; however, this requires a much steeper angle of injection, which decrease clarity of needle visualization and makes needle tracking more challenging.
- Pearls/pitfalls
  - Toe-ing in of the lateral end of the transducer or application of a beam-steering mode will improve needle visualization.
  - Color Doppler should be applied to identify the suprascapular artery above the superior transverse scapular ligament and to plan an injection course that ensures its safety.

Quadrilateral Space

Anatomy and Ultrasound Evaluation

The axillary nerve and posterior circumflex humeral artery course from the axilla anteriorly to the posterior shoulder through the quadrilateral space, which is bordered superiorly by the teres minor, inferiorly by the teres major, medially by the long head of triceps, and laterally by the humeral surgical neck. Beyond the quadrilateral space, the axillary nerve innervates the del-

toid and teres minor and provides sensation from the lateral arm.

A linear transducer is used to evaluate the quadrilateral space with the patient in a prone or sitting position and the arm internally rotated. A posterior longitudinal view of the humeral head and surgical neck is obtained with the teres minor visualized transversely. The posterior circumflex humeral artery and axillary nerve can be visualized in short axis at the inferior boarder of the teres minor at the humerus. Tracing those neurovascular structures more proximally along their course and medially, the humerus falls off and then the true quadrilateral space is visualized (Fig. 5.22). Translating more laterally, the posterior humeral circumflex artery and axillary nerve are distinctly visualized adjacent to humerus (Fig. 5.23). The transducer can then be rotated 90 degrees to evaluate the neurovascular structures in long axis.

Fig. 5.22 The posterior humeral circumflex artery (*) and axillary nerve (^) are visualized coursing between the teres minor and teres major within the quadrilateral space

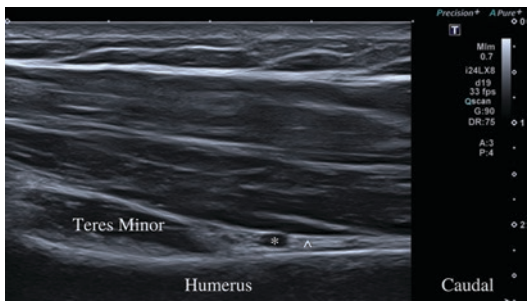

Fig. 5.23 The posterior humeral circumflex artery (*) and axillary nerve (^) are visualized adjacent to the posterior humerus, caudal from the teres minor

Pathology

Quadrilateral space syndrome (QSS) results from compression or traction of the axillary nerve (neurogenic), the posterior circumflex humeral artery (PCHA) (vascular), or both structures as they traverse the quadrilateral space. QSS is most common in volleyball [192–195], baseball [137, 196–198] (17, 18, 20, 21, 22), and swimming athletes, who perform repetitive overhead movements of abduction and external rotation [199]. Additional etiologies include mechanical compression secondary to improper crutch use or cast application, fibrous bands [200], and paralabral cysts [179], or iatrogenic injury during shoulder arthroscopy [201]. QSS with involvement of the axillary nerve will result in selective atrophy of the teres minor and sparing of deltoid, as axillary innervation to deltoid occurs proximal from the quadrilateral space. Isolated teres minor weakness and shoulder external rotation can be difficult to diagnose clinically. Ultrasound can identify isolated teres minor atrophy with an intact distal tendon, manifested as relative loss of bulk and muscular hyperechogenicity compared to the adjacent infraspinatus [184]. Ultrasound can also be used to dynamically evaluate the quadrilateral space compressive lesions or masses.

Interventional Procedures

Diagnostic axillary neural blockade within the quadrilateral space is the most common intervention at this location [202]. There are no studies to date describing the injection of an orthobiologic agent in the management of quadrilateral space syndrome. The accuracy of injection into the quadrilateral space has not been described.

Procedural protocol: Quadrilateral space/axillary perineural injection

- Patient position – Lateral decubitus on contralateral side. The affected side should be up and the affected arm fully abducted with the patient's hand resting on the back of their head.

- Transducer selection – High-frequency, linear (>10 MHz)
- Transducer position – In the axial plane, and mid-humerus. Find the long head of the triceps at the spiral groove and follow the triceps proximally into the axilla to the humeral head. Visualize the axillary nerve anterior to the inferior joint capsule.
- Needle selection – 25-gauge 2-inch needle (or larger depending on body habitus)
- Injectate selection – Anesthetize with lidocaine or Marcaine. Inject anesthetic or steroid. Typically inject 3–5 mL.
- Needle trajectory and target – In-plane, posterolateral to anteromedial through the triceps long head and targeting the axillary nerve and a perineural injection.
- Pearls/pitfalls:
  - The patient can be positioned prone, and a needle trajectory through the teres major can be taken, rather than a lateral decubitus position and approach through the long head of the triceps.

Pectoralis Major

Anatomy and Ultrasound Evaluation

The pectoralis major is a broad muscle in the anterior chest and shoulder that functions as a strong adductor and internal rotator of the shoulder. It has three heads of origin and a lateral insertion to the lateral lip of the humeral bicipital groove. The clavicular head originates from the anteromedial two thirds of the clavicle and superior sternum. The sternal head originates from the inferior sternum and costal cartilage of the medial first through fifth ribs. The abdominal head originates from the fifth and sixth ribs. Each head forms a lamina, and those laminae fuse to form a trilaminar distal tendon that twists 90 degrees just before it's insertion on the lateral lip of the bicipital groove, such that the clavicular head inserts more distally and the sternal and abdominal heads more proximally on the humerus [203]. The tendon measures about 5 cm in medial to lateral length and 4 cm in craniocaudal width [204]. The tendon of the pectoralis major has a unique U shape with the anterior fibers coming from the clavicular head and superior sternal segments and the posterior fibers coming from the inferior sternal and abdominal segments [204].

Ultrasound examination of the pectoralis major tendon at its insertion is most commonly carried out using a linear transducer with the arm abducted and externally rotated while the patient is supine. The transducer is placed in the anatomic axial plane over the bicipital groove with the bicep tendon in short axis. The transducer is then moved distally, and the pectoralis major will come into view as it courses from medial to lateral. It can be visualized in long axis coursing superficial to the coracobrachialis and biceps on its way to insert on the lateral edge of the bicipital groove (Fig. 5.24). The integrity of the tendon and the entire craniocaudal and mediolateral course should be evaluated. The tendon should have a fibrillar pattern and the superficial clavicular/sternal head and the deeper sternal/abdominal heads can be evaluated [205] (Fig. 5.25). The transducer can be moved medially to evaluate the muscle bulk as well. The muscle can be followed all the way to its origin on the clavicle, sternum, and ribs, but this is less commonly performed.

Pathology

Traumatic rupture of the pectoralis major is an uncommon sports injury that typically occurs while performing a bench press during maximal

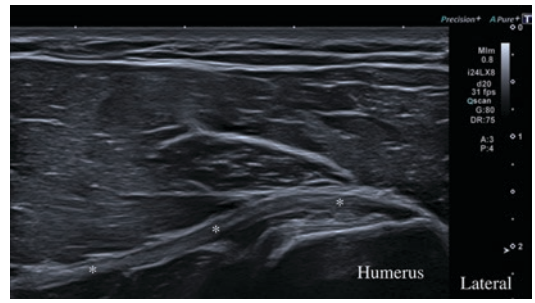

Fig. 5.24 Longitudinal view of the distal pectoralis major tendon (*) inserting onto humerus

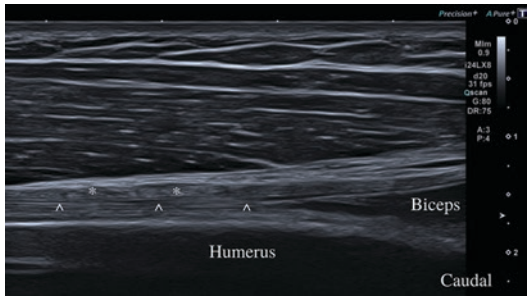

Fig. 5.25 Transverse view of the distal pectoralis major tendon (*). The long head biceps brachii tendon (^) is visualized deep to the pectoralis major tendon

Table 5.5 Anatomic classification of pectoralis major tears [209]

Type	Injury Pattern
I	Contusion or sprain
II	Partial tear
III	Complete tear
III-A	at muscle origin
III-B	at muscle belly
III-C	at myotendinous junction
III-D	at tendinous insertion

eccentric contraction with the arm in forced external rotation with extension and abduction of the humerus [206, 207]. Tear occur most commonly in active men between the ages of 20–40 [208]. Tears have historically been classified by the system described by Tietjen in 1980 (Table 5.5) [209]. Rupture most commonly occurs at the distal insertion of the inferior fibers of the sternocostal head, followed by the superior fibers of the sternocostal head or the myotendinous junction [206]. In cases of rupture, the tendon will either have a wavy appearance (if tear occurs in the muscle or near the myotendinous junction) or will not be visualized (distal tear), and edema or fluid can be seen anterior to the coracobrachialis muscle. The tendon of the pectoralis major is a stabilizer to the long head of the biceps, so when it is ruptured, the biceps tendon will be elevated off of the humerus [184]. With time, adhesions may form a pseudotendon between the retracted muscle and stump of the actual tendon [210]. Anatomic surgical repair results in better outcomes than conservative treatment alone [211].

Procedural protocol: Pectoralis major

Technique #1

- Patient position – Supine, shoulder held at side and externally rotated
- Transducer selection – High-frequency, linear (>10 MHz)
- Transducer position – In the axial plane just distal to the deltopectoral interval. Find the biceps brachii long head in its transverse plane, and track it to its myotendinous junction. Just cephalad to biceps long head myotendinous junction, the pectoralis major tendon is visualized as a laminar-appearing tendon in its longitudinal axis to its humeral insertion.
- Needle selection – 25-gauge 2-inch needle (or larger depending on body habitus and muscularity)
- Injectate selection – Anesthetize with lidocaine or Marcaine. Inject anesthetic or steroid. Typically inject 3–5 mL.
- Needle trajectory and target – In-plane, lateral to medial in plane with the tendon at its humeral insertion to perform a peritendinous injection.

Technique #

- Patient position – Supine, shoulder held at side and externally rotated
- Transducer selection – High-frequency, linear (>10 MHz)
- Transducer position – In the anatomic sagittal plane just distal to the deltopectoral interval. Find the biceps brachii long head in its longitudinal plane, and track it to its myotendinous junction. It is here the it sits deep to the tendon of pectoralis major. This plane can be translated medially to identify and to target a pectoralis major myotendinous injury.
- Needle selection – 25-gauge 2-inch needle (or larger depending on body habitus and muscularity)
- Injectate selection – Anesthetize with lidocaine or Marcaine. Inject anesthetic or steroid. Typically inject 3–5 mL.
- Needle trajectory and target – Cephalad to caudad, in an anatomic sagittal plane transverse to the pectoralis major.

References

1. Buck FM, et al. Degeneration of the long biceps tendon: comparison of MRI with gross anatomy and histology. AJR Am J Roentgenol. 2009;193(5):1367–75.
2. Buck FM, et al. Magnetic resonance histologic correlation in rotator cuff tendons. J Magn Reson Imaging. 2010;32(1):165–72.
3. Jacobson JA, et al. Full-thickness and partial-thickness supraspinatus tendon tears: value of US signs in diagnosis. Radiology. 2004;230(1):234–42.
4. Skendzel JG, et al. Long head of biceps brachii tendon evaluation: accuracy of preoperative ultrasound. AJR Am J Roentgenol. 2011;197(4):942–8.
5. Jacobson J. Fundamentals of musculoskeletal ultrasound. 3rd ed. Philadelphia: Elsevier, Inc.; 2018.
6. Bianchi S, Martinoli C. Ultrasound of the musculoskeletal system. Berlin: Springer Science & Business Media; 2007.
7. Nwawka OK, et al. Volume and movement affecting flow of Injectate between the biceps tendon sheath and Glenohumeral joint: a cadaveric study. AJR Am J Roentgenol. 2016;206(2):373–7.
8. Hollister MS, et al. Association of sonographically detected subacromial/subdeltoid bursal effusion and intraarticular fluid with rotator cuff tear. AJR Am J Roentgenol. 1995;165(3):605–8.
9. Beall DP, et al. Association of biceps tendon tears with rotator cuff abnormalities: degree of correlation with tears of the anterior and superior portions of the rotator cuff. AJR Am J Roentgenol. 2003;180(3):633–9.
10. Catapano M, et al. Effectiveness of dextrose Prolotherapy for rotator cuff tendinopathy: a systematic review. PM R. 2020;12(3):288–300.
11. Seven MM, et al. Effectiveness of prolotherapy in the treatment of chronic rotator cuff lesions. Orthop Traumatol Surg Res. 2017;103(3):427–33.
12. Ibrahim VM, et al. Use of platelet rich plasma for the treatment of bicipital tendinopathy in spinal cord injury:: a pilot study. Top Spinal Cord Inj Rehabil. 2012;18(1):77–8.
13. Petchprapa CN, et al. The rotator interval: a review of anatomy, function, and normal and abnormal MRI appearance. AJR Am J Roentgenol. 2010;195(3):567–76.
14. Gazzillo GP, et al. Accuracy of palpating the long head of the biceps tendon: an ultrasonographic study. PM R. 2011;3(11):1035–40.
15. Aly AR, Rajasekaran S, Ashworth N. Ultrasound-guided shoulder girdle injections are more accurate and more effective than landmark-guided injections: a systematic review and meta-analysis. Br J Sports Med. 2015;49(16):1042–9.
16. Hashiuchi T, et al. Accuracy of the biceps tendon sheath injection: ultrasound-guided or unguided injection? A randomized controlled trial. J Shoulder Elb Surg. 2011;20(7):1069–73.
17. Yiannakopoulos CK, et al. Ultrasound-guided versus palpation-guided corticosteroid injections for tendinosis of the long head of the biceps: a randomized comparative study. Skelet Radiol. 2020;49(4):585–91.
18. Kim SY, et al. Three-dimensional study of the musculotendinous architecture of supraspinatus and its functional correlations. Clin Anat. 2007;20(6):648–55.
19. Vahlensieck M, Haack K a, Schmidt HM. Two portions of the supraspinatus muscle: a new finding about the muscles macroscopy by dissection and magnetic resonance imaging. Surg Radiol Anat. 1994;16(1):101–4.
20. Ferri M, et al. Sonography of full-thickness supraspinatus tears: comparison of patient positioning technique with surgical correlation. AJR Am J Roentgenol. 2005;184(1):180–4.
21. Ruotolo C, Fow JE, Nottage WM. The supraspinatus footprint: an anatomic study of the supraspinatus insertion. Arthroscopy. 2004;20(3):246–9.
22. Bretzke CA, et al. Ultrasonography of the rotator cuff. Normal and pathologic anatomy. Investig Radiol. 1985;20(3):311–5.
23. Karthikeyan S, et al. Ultrasound dimensions of the rotator cuff in young healthy adults. J Shoulder Elb Surg. 2014;23(8):1107–12.
24. Kim K, et al. Ultrasound dimensions of the rotator cuff and other associated structures in Korean healthy adults. J Korean Med Sci. 2016;31(9):1472–8.
25. Schaeffeler C, et al. Tears at the rotator cuff footprint: prevalence and imaging characteristics in 305 MR arthrograms of the shoulder. Eur Radiol. 2011;21(7):1477–84.
26. de Jesus JO, et al. Accuracy of MRI, MR arthrography, and ultrasound in the diagnosis of rotator cuff tears: a meta-analysis. AJR Am J Roentgenol. 2009;192(6):1701–7.
27. Roy JS, et al. Diagnostic accuracy of ultrasonography, MRI and MR arthrography in the characterisation of rotator cuff disorders: a systematic review and meta-analysis. Br J Sports Med. 2015;49(20):1316–28.
28. Kim HM, et al. Location and initiation of degenerative rotator cuff tears: an analysis of three hundred and sixty shoulders. J Bone Joint Surg Am. 2010;92(5):1088–96.
29. van Holsbeeck MT, et al. US depiction of partial-thickness tear of the rotator cuff. Radiology. 1995;197(2):443–6.
30. Chianca V, et al. Rotator cuff calcific tendinopathy: from diagnosis to treatment. Acta Biomed. 2018;89(1-s):186–96.
31. Sansone V, et al. Calcific tendinopathy of the shoulder: clinical perspectives into the mechanisms, pathogenesis, and treatment. Orthop Res Rev. 2018;10:63–72.
32. Uhthoff HK, Loehr JW. Calcific tendinopathy of the rotator cuff: pathogenesis, diagnosis, and management. J Am Acad Orthop Surg. 1997;5(4):183–91.

33. Hackett L, et al. Are the symptoms of calcific tendinitis due to Neoinnervation and/or neovascularization? J Bone Joint Surg Am. 2016;98(3):186–92.
34. Chiou HJ, et al. The role of high-resolution ultrasonography in management of calcific tendonitis of the rotator cuff. Ultrasound Med Biol. 2001;27(6):735–43.
35. Farin PU. Consistency of rotator-cuff calcifications. Observations on plain radiography, sonography, computed tomography, and at needle treatment. Investig Radiol. 1996;31(5):300–4.
36. Gärtner J, Heyer A. Calcific tendinitis of the shoulder. Orthopade. 1995;24(3):284–302.
37. Molé D, et al. Results of endoscopic treatment of non-broken tendinopathies of the rotator cuff. 2. Calcifications of the rotator cuff. Rev Chir Orthop Reparatrice Appar Mot. 1993;79(7):532–41.
38. Dean BJ, et al. The risks and benefits of glucocorticoid treatment for tendinopathy: a systematic review of the effects of local glucocorticoid on tendon. Semin Arthritis Rheum. 2014;43(4):570–6.
39. Castricini R, et al. Platelet-rich plasma augmentation for arthroscopic rotator cuff repair: a randomized controlled trial. Am J Sports Med. 2011;39(2):258–65.
40. Flury M, et al. Does pure platelet-rich plasma affect postoperative clinical outcomes after arthroscopic rotator cuff repair? A randomized controlled trial. Am J Sports Med. 2016;44(8):2136–46.
41. Jo CH, et al. Does platelet-rich plasma accelerate recovery after rotator cuff repair? A prospective cohort study. Am J Sports Med. 2011;39(10):2082–90.
42. Malavolta EA, et al. Platelet-rich plasma in rotator cuff repair: a prospective randomized study. Am J Sports Med. 2014;42(10):2446–54.
43. Randelli P, et al. Platelet rich plasma in arthroscopic rotator cuff repair: a prospective RCT study, 2-year follow-up. J Shoulder Elb Surg. 2011;20(4):518–28.
44. Carr JB 2nd, Rodeo SA. The role of biologic agents in the management of common shoulder pathologies: current state and future directions. J Shoulder Elb Surg. 2019;28(11):2041–52.
45. Zhang Q, et al. Are platelet-rich products necessary during the arthroscopic repair of full-thickness rotator cuff tears: a meta-analysis. PLoS One. 2013;8(7):e69731.
46. Wang A, et al. Do postoperative platelet-rich plasma injections accelerate early tendon healing and functional recovery after arthroscopic supraspinatus repair? A randomized controlled trial. Am J Sports Med. 2015;43(6):1430–7.
47. Moraes VY, et al. Platelet-rich therapies for musculoskeletal soft tissue injuries. Cochrane Database Syst Rev. 2013;12:Cd010071.
48. Schwitzguebel AJ, et al. Efficacy of platelet-rich plasma for the treatment of interstitial supraspinatus tears: a double-blinded, randomized controlled trial. Am J Sports Med. 2019;47(8):1885–92.
49. Rha DW, et al. Comparison of the therapeutic effects of ultrasound-guided platelet-rich plasma injection and dry needling in rotator cuff disease: a randomized controlled trial. Clin Rehabil. 2013;27(2):113–22.
50. Kesikburun S, et al. Platelet-rich plasma injections in the treatment of chronic rotator cuff tendinopathy: a randomized controlled trial with 1-year follow-up. Am J Sports Med. 2013;41(11):2609–16.
51. Lin MT, et al. Comparative effectiveness of injection therapies in rotator cuff tendinopathy: a systematic review, pairwise and network meta-analysis of randomized controlled trials. Arch Phys Med Rehabil. 2019;100(2):336–349.e15.
52. Mautner K, et al. A call for a standard classification system for future biologic research: the rationale for new PRP nomenclature. PM R. 2015;7(4 Suppl):S53–s59.
53. Kim SJ, et al. Effect of platelet-rich plasma on the degenerative rotator cuff tendinopathy according to the compositions. J Orthop Surg Res. 2019;14(1):408.
54. Cole B, et al. Ultrasound-guided injections for supraspinatus tendinopathy: corticosteroid versus glucose prolotherapy - a randomized controlled clinical trial. Shoulder Elbow. 2018;10(3):170–8.
55. George J, et al. Comparative effectiveness of ultrasound-guided Intratendinous Prolotherapy injection with conventional treatment to treat focal supraspinatus tendinosis. Scientifica (Cairo). 2018;2018:4384159.
56. Lin CL, Huang CC, Huang SW. Effects of hypertonic dextrose injection in chronic supraspinatus tendinopathy of the shoulder: a randomized placebo-controlled trial. Eur J Phys Rehabil Med. 2019;55(4):480–7.
57. Osti L, et al. Clinical evidence in the treatment of rotator cuff tears with hyaluronic acid. Muscles Ligaments Tendons J. 2015;5(4):270–5.
58. Cai YU, et al. Sodium hyaluronate and platelet-rich plasma for partial-thickness rotator cuff tears. Med Sci Sports Exerc. 2019;51(2):227–33.
59. Wu PT, et al. Intratendinous injection of hyaluronate induces acute inflammation: a possible detrimental effect. PLoS One. 2016;11(5):e0155424.
60. Kim SJ, et al. Effects of bone marrow aspirate concentrate and platelet-rich plasma on patients with partial tear of the rotator cuff tendon. J Orthop Surg Res. 2018;13(1):1.
61. Jo CH, et al. Intratendinous injection of autologous adipose tissue-derived mesenchymal stem cells for the treatment of rotator cuff disease: a first-in-human trial. Stem Cells. 2018;36(9):1441–50.
62. Finnoff JT, et al. Treatment of chronic tendinopathy with ultrasound-guided needle tenotomy and platelet-rich plasma injection. PM R. 2011;3(10):900–11.
63. Gatt DL, Charalambous CP. Ultrasound-guided barbotage for calcific tendonitis of the shoulder: a systematic review including 908 patients. Arthroscopy. 2014;30(9):1166–72.
64. de Witte PB, et al. Rotator cuff calcific tendinitis: ultrasound-guided needling and lavage versus subacromial corticosteroids: five-year outcomes of

a randomized controlled trial. Am J Sports Med. 2017;45(14):3305–14.
65. de Witte PB, et al. Calcific tendinitis of the rotator cuff: a randomized controlled trial of ultrasound-guided needling and lavage versus subacromial corticosteroids. Am J Sports Med. 2013;41(7):1665–73.
66. Morag Y, et al. The subscapularis: anatomy, injury, and imaging. Skelet Radiol. 2011;40(3):255–69.
67. Radas CB, Pieper HG. The coracoid impingement of the subscapularis tendon: a cadaver study. J Shoulder Elb Surg. 2004;13(2):154–9.
68. Navarro-Ledesma S, et al. Is coracohumeral distance associated with pain-function, and shoulder range of movement, in chronic anterior shoulder pain? BMC Musculoskelet Disord. 2017;18(1):136.
69. Sansone V, et al. Calcific tendinopathy of the rotator cuff: the correlation between pain and imaging features in symptomatic and asymptomatic female shoulders. Skelet Radiol. 2016;45(1):49–55.
70. Fessa CK, et al. Posterosuperior glenoid internal impingement of the shoulder in the overhead athlete: pathogenesis, clinical features and MR imaging findings. J Med Imaging Radiat Oncol. 2015;59(2):182–7.
71. Tirman PF, et al. Posterosuperior glenoid impingement of the shoulder: findings at MR imaging and MR arthrography with arthroscopic correlation. Radiology. 1994;193(2):431–6.
72. Friend J, et al. Teres minor innervation in the context of isolated muscle atrophy. Surg Radiol Anat. 2010;32(3):243–9.
73. Kang Y, et al. The pattern of idiopathic isolated teres minor atrophy with regard to its two-bundle anatomy. Skelet Radiol. 2019;48(3):363–74.
74. Beals TC, Harryman DT 2nd, Lazarus MD. Useful boundaries of the subacromial bursa. Arthroscopy. 1998;14(5):465–70.
75. Birnbaum K, Lierse W. Anatomy and function of the bursa subacromialis. Acta Anat (Basel). 1992;145(4):354–63.
76. Kennedy MS, Nicholson HD, Woodley SJ. Clinical anatomy of the subacromial and related shoulder bursae: a review of the literature. Clin Anat. 2017;30(2):213–26.
77. Duranthon LD, Gagey OJ. Anatomy and function of the subdeltoid bursa. Surg Radiol Anat. 2001;23(1):23–5.
78. van Holsbeeck M, Strouse PJ. Sonography of the shoulder: evaluation of the subacromial-subdeltoid bursa. AJR Am J Roentgenol. 1993;160(3):561–4.
79. Michener LA, et al. Supraspinatus tendon and subacromial space parameters measured on ultrasonographic imaging in subacromial impingement syndrome. Knee Surg Sports Traumatol Arthrosc. 2015;23(2):363–9.
80. Bureau NJ, et al. Dynamic sonography evaluation of shoulder impingement syndrome. AJR Am J Roentgenol. 2006;187(1):216–20.
81. Beard DJ, et al. Arthroscopic subacromial decompression for subacromial shoulder pain (CSAW): a multicentre, pragmatic, parallel group, placebo-controlled, three-group, randomised surgical trial. Lancet. 2018;391(10118):329–38.
82. Haahr JP, et al. Exercises versus arthroscopic decompression in patients with subacromial impingement: a randomised, controlled study in 90 cases with a one year follow up. Ann Rheum Dis. 2005;64(5):760–4.
83. Wu T, et al. Ultrasound-guided versus blind subacromial-subdeltoid bursa injection in adults with shoulder pain: a systematic review and meta-analysis. Semin Arthritis Rheum. 2015;45(3):374–8.
84. Nejati P, et al. Treatment of subacromial impingement syndrome: platelet-rich plasma or exercise therapy? A randomized controlled trial. Orthop J Sports Med. 2017;5(5):2325967117702366.
85. Say F, Gurler D, Bulbul M. Platelet-rich plasma versus steroid injection for subacromial impingement syndrome. J Orthop Surg (Hong Kong). 2016;24(1):62–6.
86. Schneider A, et al. Platelet-rich plasma and the shoulder: clinical indications and outcomes. Curr Rev Musculoskelet Med. 2018;11(4):593–7.
87. Rutten MJ, et al. Injection of the subacromial-subdeltoid bursa: blind or ultrasound-guided? Acta Orthop. 2007;78(2):254–7.
88. Dogu B, et al. Blind or ultrasound-guided corticosteroid injections and short-term response in subacromial impingement syndrome: a randomized, double-blind, prospective study. Am J Phys Med Rehabil. 2012;91(8):658–65.
89. Ahn KS, et al. Ultrasound elastography of lateral epicondylosis: clinical feasibility of quantitative elastographic measurements. AJR Am J Roentgenol. 2014;202(5):1094–9.
90. Mathews PV, Glousman RE. Accuracy of subacromial injection: anterolateral versus posterior approach. J Shoulder Elb Surg. 2005;14(2):145–8.
91. Partington PF, Broome GH. Diagnostic injection around the shoulder: hit and miss? A cadaveric study of injection accuracy. J Shoulder Elb Surg. 1998;7(2):147–50.
92. Eustace JA, et al. Comparison of the accuracy of steroid placement with clinical outcome in patients with shoulder symptoms. Ann Rheum Dis. 1997;56(1):59–63.
93. Mazzocca AD, Arciero RA, Bicos J. Evaluation and treatment of acromioclavicular joint injuries. Am J Sports Med. 2007;35(2):316–29.
94. Petersson CJ, Redlund-Johnell I. Radiographic joint space in normal acromioclavicular joints. Acta Orthop Scand. 1983;54(3):431–3.
95. Mall NA, et al. Degenerative joint disease of the acromioclavicular joint: a review. Am J Sports Med. 2013;41(11):2684–92.
96. Saccomanno MF, Ieso CDE, Milano G. Acromioclavicular joint instability: anatomy, biomechanics and evaluation. Joints. 2014;2(2):87–92.
97. Chronopoulos E, et al. Diagnostic value of physical tests for isolated chronic acromioclavicular lesions. Am J Sports Med. 2004;32(3):655–61.

98. Jacobson JA. Fundamentals of musculoskeletal ultrasound E-book. Philadelphia: Elsevier Health Sciences; 2017.
99. Hobusch GM, et al. Ultrasound of horizontal instability of the acromioclavicular joint : a simple and reliable test based on a cadaveric study. Wien Klin Wochenschr. 2019;131(3-4):81–6.
100. Sammarco VJ. Os acromiale: frequency, anatomy, and clinical implications. J Bone Joint Surg Am. 2000;82(3):394–400.
101. Boehm TD, et al. Ultrasonographic appearance of os acromiale. Ultraschall Med. 2003;24(3):180–3.
102. Armstrong A. Evaluation and management of adult shoulder pain: a focus on rotator cuff disorders, acromioclavicular joint arthritis, and glenohumeral arthritis. Med Clin North Am. 2014;98(4):755–75. xii
103. Jacob AK, Sallay PI. Therapeutic efficacy of corticosteroid injections in the acromioclavicular joint. Biomed Sci Instrum. 1997;34:380–5.
104. Chang Chien GC, et al. Ultrasonography leads to accurate diagnosis and management of painful acromioclavicular joint cyst. Pain Pract. 2015;15(7):E72–5.
105. Mikell C, Gelber J, Nagdev A. Ultrasound-guided analgesic injection for acromioclavicular joint separation in the emergency department. Am J Emerg Med. 2020;38(1):162.e3–5.
106. van Riet RP, Goehre T, Bell SN. The long term effect of an intra-articular injection of corticosteroids in the acromioclavicular joint. J Shoulder Elb Surg. 2012;21(3):376–9.
107. Gokkus K, et al. Limited distal clavicle excision of acromioclavicular joint osteoarthritis. Orthop Traumatol Surg Res. 2016;102(3):311–8.
108. Hsieh PC, et al. Ultrasound-guided Prolotherapy for acromial Enthesopathy and acromioclavicular joint Arthropathy: a single-arm prospective study. J Ultrasound Med. 2019;38(3):605–12.
109. Borbas P, et al. The influence of ultrasound guidance in the rate of success of acromioclavicular joint injection: an experimental study on human cadavers. J Shoulder Elb Surg. 2012;21(12):1694–7.
110. Sabeti-Aschraf M, et al. Ultrasound guidance improves the accuracy of the acromioclavicular joint infiltration: a prospective randomized study. Knee Surg Sports Traumatol Arthrosc. 2011;19(2):292–5.
111. Scillia A, et al. Accuracy of in vivo palpation-guided acromioclavicular joint injection assessed with contrast material and fluoroscopic evaluations. Skelet Radiol. 2015;44(8):1135–9.
112. Wasserman BR, et al. Accuracy of acromioclavicular joint injections. Am J Sports Med. 2013;41(1):149–52.
113. van Tongel A, et al. A cadaveric study of the structural anatomy of the sternoclavicular joint. Clin Anat. 2012;25(7):903–10.
114. Bearn JG. Direct observations on the function of the capsule of the sternoclavicular joint in clavicular support. J Anat. 1967;101(Pt 1):159–70.
115. Brossmann J, et al. Sternoclavicular joint: MR imaging—anatomic correlation. Radiology. 1996;198(1):193–8.
116. Yood RA, Goldenberg DL. Sternoclavicular joint arthritis. Arthritis Rheum. 1980;23(2):232–9.
117. Stein A, McAleer S, Hinz M. Microperforation prolotherapy: a novel method for successful nonsurgical treatment of atraumatic spontaneous anterior sternoclavicular subluxation, with an illustrative case. Open Access J Sports Med. 2011;2:47–52.
118. Peterson CK, et al. CT-guided sternoclavicular joint injections: description of the procedure, reliability of imaging diagnosis, and short-term patient responses. AJR Am J Roentgenol. 2010;195(6):W435–9.
119. Taneja AK, et al. Diagnostic yield of CT-guided sampling in suspected sternoclavicular joint infection. Skelet Radiol. 2013;42(4):479–85.
120. Galla R, et al. Sternoclavicular steroid injection for treatment of pain in a patient with osteitis condensans of the clavicle. Pain Physician. 2009;12(6):987–90.
121. Pourcho AM, Sellon JL, Smith J. Sonographically guided sternoclavicular joint injection: description of technique and validation. J Ultrasound Med. 2015;34(2):325–31.
122. Middleton WD, et al. Pitfalls of rotator cuff sonography. AJR Am J Roentgenol. 1986;146(3):555–60.
123. Taljanovic MS, et al. Sonography of the glenoid labrum: a cadaveric study with arthroscopic correlation. AJR Am J Roentgenol. 2000;174(6):1717–22.
124. Ogul H, et al. Sonoarthrographic examination of posterior labrocapsular structures of the shoulder joint. Br J Radiol. 2020;93(1106):20190886.
125. Park D. Evaluation of Posterosuperior labral tear with shoulder sonography after intra-articular injection: a case series. Am J Phys Med Rehabil. 2017;96(3):e48–51.
126. Boswell B, et al. Emergency medicine resident-driven point of care ultrasound for suspected shoulder dislocation. South Med J. 2019;112(12):605–9.
127. Abbasi S, et al. Diagnostic accuracy of ultrasonographic examination in the management of shoulder dislocation in the emergency department. Ann Emerg Med. 2013;62(2):170–5.
128. Khoury V, Van Lancker HP, Martineau PA. Sonography as a tool for identifying engaging hill-Sachs lesions: preliminary experience. J Ultrasound Med. 2013;32(9):1653–7.
129. Kerr R, et al. Osteoarthritis of the glenohumeral joint: a radiologic-pathologic study. AJR Am J Roentgenol. 1985;144(5):967–72.
130. Crowell MS, Tragord BS. Orthopaedic manual physical therapy for shoulder pain and impaired movement in a patient with glenohumeral joint osteoarthritis: a case report. J Orthop Sports Phys Ther. 2015;45(6):453–61. a1-3
131. Saltzman BM, et al. Glenohumeral osteoarthritis in the young patient. J Am Acad Orthop Surg. 2018;26(17):e361–70.
132. van der Meijden OA, Gaskill TR, Millett PJ. Glenohumeral joint preservation: a review of

management options for young, active patients with osteoarthritis. Adv Orthop. 2012;2012:160923.
133. Sayegh ET, et al. Surgical treatment options for Glenohumeral arthritis in young patients: a systematic review and meta-analysis. Arthroscopy. 2015;31(6):1156–1166.e8.
134. Ryu KN, et al. Adhesive capsulitis of the shoulder joint: usefulness of dynamic sonography. J Ultrasound Med. 1993;12(8):445–9.
135. Lee JC, et al. Adhesive capsulitis: sonographic changes in the rotator cuff interval with arthroscopic correlation. Skelet Radiol. 2005;34(9):522–7.
136. Homsi C, et al. Ultrasound in adhesive capsulitis of the shoulder: is assessment of the coracohumeral ligament a valuable diagnostic tool? Skelet Radiol. 2006;35(9):673–8.
137. Redler LH, Dennis ER. Treatment of adhesive capsulitis of the shoulder. J Am Acad Orthop Surg. 2019;27(12):e544–54.
138. Struyf F, Meeus M. Current evidence on physical therapy in patients with adhesive capsulitis: what are we missing? Clin Rheumatol. 2014;33(5):593–600.
139. Lee S, et al. The effects of extracorporeal shock wave therapy on pain and range of motion in patients with adhesive capsulitis. J Phys Ther Sci. 2017;29(11):1907–9.
140. Saltychev M, et al. Effectiveness of Hydrodilatation in adhesive capsulitis of shoulder: a systematic review and meta-analysis. Scand J Surg. 2018;107(4):285–93.
141. Griesser MJ, et al. Adhesive capsulitis of the shoulder: a systematic review of the effectiveness of intra-articular corticosteroid injections. J Bone Joint Surg Am. 2011;93(18):1727–33.
142. Jain TK, Sharma NK. The effectiveness of physiotherapeutic interventions in treatment of frozen shoulder/adhesive capsulitis: a systematic review. J Back Musculoskelet Rehabil. 2014;27(3):247–73.
143. Porcellini G, et al. Intra-articular glenohumeral injections of HYADD(R)4-G for the treatment of painful shoulder osteoarthritis: a prospective multicenter, open-label trial. Joints. 2015;3(3):116–21.
144. Silverstein E, Leger R, Shea KP. The use of intra-articular hylan G-F 20 in the treatment of symptomatic osteoarthritis of the shoulder: a preliminary study. Am J Sports Med. 2007;35(6):979–85.
145. Noel E, et al. Efficacy and safety of Hylan G-F 20 in shoulder osteoarthritis with an intact rotator cuff. Open-label prospective multicenter study. Joint Bone Spine. 2009;76(6):670–3.
146. Di Giacomo G, de Gasperis N. Hyaluronic acid intra-articular injections in patients affected by moderate to severe Glenohumeral osteoarthritis: a prospective randomized study. Joints. 2017;5(3):138–42.
147. McKee MD, et al. NASHA hyaluronic acid for the treatment of shoulder osteoarthritis: a prospective, single-arm clinical trial. Med Devices (Auckl). 2019;12:227–34.
148. Merolla G, et al. Efficacy of Hylan G-F 20 versus 6-methylprednisolone acetate in painful shoulder osteoarthritis: a retrospective controlled trial. Musculoskelet Surg. 2011;95(3):215–24.
149. Kwon YW, Eisenberg G, Zuckerman JD. Sodium hyaluronate for the treatment of chronic shoulder pain associated with glenohumeral osteoarthritis: a multicenter, randomized, double-blind, placebo-controlled trial. J Shoulder Elb Surg. 2013;22(5):584–94.
150. Blaine T, et al. Treatment of persistent shoulder pain with sodium hyaluronate: a randomized, controlled trial. A multicenter study. J Bone Joint Surg Am. 2008;90(5):970–9.
151. Centeno CJ, et al. A prospective multi-site registry study of a specific protocol of autologous bone marrow concentrate for the treatment of shoulder rotator cuff tears and osteoarthritis. J Pain Res. 2015;8:269–76.
152. Striano RD, et al. Refractory shoulder pain with osteoarthritis, and rotator cuff tear, treated with micro-fragmented adipose tissue. J Orthop Spine Sports Med. 2018;2(1):014.
153. Jong BY, Goel DP. Biologic options for Glenohumeral arthritis. Clin Sports Med. 2018;37(4):537–48.
154. Wang W, et al. Effectiveness of corticosteroid injections in adhesive capsulitis of shoulder: a meta-analysis. Medicine (Baltimore). 2017;96(28):e7529.
155. Xiao RC, et al. Corticosteroid injections for adhesive capsulitis: a review. Clin J Sport Med. 2017;27(3):308–20.
156. Paruthikunnan SM, et al. Intra-articular steroid for adhesive capsulitis: does hydrodilatation give any additional benefit? A randomized control trial. Skelet Radiol. 2019.
157. Yoon SH, et al. Optimal dose of intra-articular corticosteroids for adhesive capsulitis: a randomized, triple-blind, placebo-controlled trial. Am J Sports Med. 2013;41(5):1133–9.
158. Shang X, et al. Intra-articular versus subacromial corticosteroid injection for the treatment of adhesive capsulitis: a meta-analysis and systematic review. Biomed Res Int. 2019;2019:1274790.
159. Kim YS, et al. Comparison of high- and low-dose intra-articular triamcinolone acetonide injection for treatment of primary shoulder stiffness: a prospective randomized trial. J Shoulder Elb Surg. 2017;26(2):209–15.
160. Prestgaard T, et al. Ultrasound-guided intra-articular and rotator interval corticosteroid injections in adhesive capsulitis of the shoulder: a double-blind, sham-controlled randomized study. Pain. 2015;156(9):1683–91.
161. Ogul H, et al. Ultrasound-guided shoulder MR arthrography: comparison of rotator interval and posterior approach. Clin Imaging. 2014;38(1):11–7.
162. Sun Y, et al. The effect of corticosteroid injection into rotator interval for early frozen shoulder: a randomized controlled trial. Am J Sports Med. 2018;46(3):663–70.
163. Barman A, et al. Single intra-articular platelet-rich plasma versus corticosteroid injections in the treat-

ment of adhesive capsulitis of the shoulder: a cohort study. Am J Phys Med Rehabil. 2019;98(7):549–57.
164. Lin J. Platelet-rich plasma injection in the treatment of frozen shoulder: a randomized controlled trial with 6-month follow-up. Int J Clin Pharmacol Ther. 2018;56(8):366–71.
165. Sethi PM, Kingston S, Elattrache N. Accuracy of anterior intra-articular injection of the glenohumeral joint. Arthroscopy. 2005;21(1):77–80.
166. Shao X, et al. Transcoracoacromial ligament Glenohumeral injection technique: accuracy of 116 injections in idiopathic adhesive capsulitis. Arthroscopy. 2018;34(8):2337–44.
167. Catalano OA, et al. MR arthrography of the glenohumeral joint: modified posterior approach without imaging guidance. Radiology. 2007;242(2):550–4.
168. Patel DN, et al. Comparison of ultrasound-guided versus blind glenohumeral injections: a cadaveric study. J Shoulder Elb Surg. 2012;21(12):1664–8.
169. Esenyel CZ, et al. Accuracy of anterior glenohumeral injections: a cadaver study. Arch Orthop Trauma Surg. 2010;130(3):297–300.
170. Souza PM, et al. Arthrography of the shoulder: a modified ultrasound guided technique of joint injection at the rotator interval. Eur J Radiol. 2010;74(3):e29–32.
171. Choudur HN, Ellins ML. Ultrasound-guided gadolinium joint injections for magnetic resonance arthrography. J Clin Ultrasound. 2011;39(1):6–11.
172. Gokalp G, Dusak A, Yazici Z. Efficacy of ultrasonography-guided shoulder MR arthrography using a posterior approach. Skelet Radiol. 2010;39(6):575–9.
173. Ogul H, et al. Magnetic resonance arthrography of the glenohumeral joint: ultrasonography-guided technique using a posterior approach. Eurasian J Med. 2012;44(2):73–8.
174. Plancher KD, et al. The spinoglenoid ligament. Anatomy, morphology, and histological findings. J Bone Joint Surg Am. 2005;87(2):361–5.
175. Aktekin M, et al. The significance of the neurovascular structures passing through the spinoglenoid notch. Neurosciences (Riyadh). 2003;8(4):222–4.
176. Lichtenberg S, Magosch P, Habermeyer P. Compression of the suprascapular nerve by a ganglion cyst of the spinoglenoid notch: the arthroscopic solution. Knee Surg Sports Traumatol Arthrosc. 2004;12(1):72–9.
177. Steinwachs MR, et al. A ganglion of the spinoglenoid notch. J Shoulder Elb Surg. 1998;7(5):550–4.
178. Phillips CJ, Field AC, Field LD. Transcapsular decompression of shoulder ganglion cysts. Arthrosc Tech. 2018;7(12):e1263–7.
179. Tung GA, et al. MR imaging and MR arthrography of paraglenoid labral cysts. AJR Am J Roentgenol. 2000;174(6):1707–15.
180. Ferretti A, De Carli A, Fontana M. Injury of the suprascapular nerve at the spinoglenoid notch. The natural history of infraspinatus atrophy in volleyball players. Am J Sports Med. 1998;26(6):759–63.
181. Chiou HJ, et al. Alternative and effective treatment of shoulder ganglion cyst: ultrasonographically guided aspiration. J Ultrasound Med. 1999;18(8):531–5.
182. Sangam MR, et al. A study on the morphology of the suprascapular notch and its distance from the glenoid cavity. J Clin Diagn Res. 2013;7(2):189–92.
183. Rengachary SS, et al. Suprascapular entrapment neuropathy: a clinical, anatomical, and comparative study. Part 2: anatomical study. Neurosurgery. 1979;5(4):447–51.
184. Martinoli C, et al. US of the shoulder: non-rotator cuff disorders. Radiographics. 2003;23(2):381–401. quiz 534
185. Boykin RE, et al. Suprascapular neuropathy. J Bone Joint Surg Am. 2010;92(13):2348–64.
186. Urguden M, et al. Is there any effect of suprascapular notch type in iatrogenic suprascapular nerve lesions? An anatomical study. Knee Surg Sports Traumatol Arthrosc. 2004;12(3):241–5.
187. Bayramoglu A, et al. Variations in anatomy at the suprascapular notch possibly causing suprascapular nerve entrapment: an anatomical study. Knee Surg Sports Traumatol Arthrosc. 2003;11(6):393–8.
188. Blasco L, et al. Ultrasound-guided proximal and distal suprascapular nerve blocks: a comparative cadaveric study. Pain Med. 2019;21(6):1240–7.
189. Taskaynatan MA, et al. Accuracy of ultrasound-guided suprascapular nerve block measured with neurostimulation. Rheumatol Int. 2012;32(7):2125–8.
190. Laumonerie P, et al. Ultrasound-guided versus landmark-based approach to the distal suprascapular nerve block: a comparative cadaveric study. Arthroscopy. 2019;35(8):2274–81.
191. Laumonerie P, et al. Distal suprascapular nerve block-do it yourself: cadaveric feasibility study. J Shoulder Elb Surg. 2019;28(7):1291–7.
192. van de Pol D, et al. High prevalence of self-reported symptoms of digital ischemia in elite male volleyball players in the Netherlands: a cross-sectional national survey. Am J Sports Med. 2012;40(10):2296–302.
193. Vlychou M, et al. Embolisation of a traumatic aneurysm of the posterior circumflex humeral artery in a volleyball player. Br J Sports Med. 2001;35(2):136–7.
194. Atema JJ, et al. Posterior circumflex humeral artery injury with distal embolisation in professional volleyball players: a discussion of three cases. Eur J Vasc Endovasc Surg. 2012;44(2):195–8.
195. Reekers JA, et al. Traumatic aneurysm of the posterior circumflex humeral artery: a volleyball player's disease? J Vasc Interv Radiol. 1993;4(3):405–8.
196. Ligh CA, Schulman BL, Safran MR. Case reports: unusual cause of shoulder pain in a collegiate baseball player. Clin Orthop Relat Res. 2009;467(10):2744–8.
197. Kee ST, et al. Ischemia of the throwing hand in major league baseball pitchers: embolic occlusion from aneurysms of axillary artery branches. J Vasc Interv Radiol. 1995;6(6):979–82.

198. Nuber GW, et al. Arterial abnormalities of the shoulder in athletes. Am J Sports Med. 1990;18(5):514–9.
199. McClelland D, Hoy G. A case of quadrilateral space syndrome with involvement of the long head of the triceps. Am J Sports Med. 2008;36(8):1615–7.
200. Perlmutter GS. Axillary nerve injury. Clin Orthop Relat Res. 1999;368:28–36.
201. Lo IK, Burkhart SS, Parten PM. Surgery about the coracoid: neurovascular structures at risk. Arthroscopy. 2004;20(6):591–5.
202. Chen H, Narvaez VR. Ultrasound-guided quadrilateral space block for the diagnosis of quadrilateral syndrome. Case Rep Orthop. 2015;2015:378627.
203. Wolfe SW, Wickiewicz TL, Cavanaugh JT. Ruptures of the pectoralis major muscle. An anatomic and clinical analysis. Am J Sports Med. 1992;20(5):587–93.
204. Fung L, et al. Three-dimensional study of pectoralis major muscle and tendon architecture. Clin Anat. 2009;22(4):500–8.
205. Lee YK, et al. US and MR imaging of pectoralis major injuries. Radiographics. 2017;37(1):176–89.
206. Chiavaras MM, et al. Pectoralis major tears: anatomy, classification, and diagnosis with ultrasound and MR imaging. Skelet Radiol. 2015;44(2):157–64.
207. Provencher MT, et al. Injuries to the pectoralis major muscle: diagnosis and management. Am J Sports Med. 2010;38(8):1693–705.
208. ElMaraghy AW, Devereaux MW. A systematic review and comprehensive classification of pectoralis major tears. J Shoulder Elb Surg. 2012;21(3):412–22.
209. Tietjen R. Closed injuries of the pectoralis major muscle. J Trauma. 1980;20(3):262–4.
210. Rehman A, Robinson P. Sonographic evaluation of injuries to the pectoralis muscles. AJR Am J Roentgenol. 2005;184(4):1205–11.
211. Kircher J, et al. Surgical and nonsurgical treatment of total rupture of the pectoralis major muscle in athletes: update and critical appraisal. Open Access J Sports Med. 2010;1:201–5.